INTERNATIONAL JOURNAL OF CRITICAL INFRASTRUCTURE PROTECTION 24 (2019) 144–165

Available online at www.sciencedirect.com

ScienceDirect

journal homepage: www.elsevier.com/locate/IJCIP

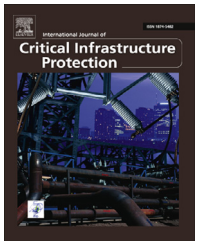

Interdependent Critical Infrastructure Model (ICIM): An agent-based model of power and water infrastructure

James R. Thompson[1,*], *Damon Frezza*[1], *Burhan Necioglu*[1], *Michael L. Cohen*[1], *Kenneth Hoffman*[1], *Kristine Rosfjord*[1]

The MITRE Corporation, 7515 Colshire Drive, McLean VA 22102, United States

ARTICLE INFO

Article history:
Received 30 May 2018
Revised 23 November 2018
Accepted 20 December 2018
Available online 23 December 2018

Keywords:
Critical infrastructure
Agent-based model
Long-term planning

ABSTRACT

The comfort, mobility, and economic well-being of a population depends on reliable and affordable electric power services, which in turn requires a sustainable water supply. It is therefore increasingly important to analyze the sustainability and resilience of mid- and long-term electric utility and water system capacity expansion plans. Due to the inherent interdependency between power and water critical infrastructure, these expansion plans should be analyzed with respect to potential challenges posed by climate change and other risks. Decision-makers therefore require tools that facilitate an integrated analysis that captures the interdependency of power and water to better inform future expansion plans. Here we develop an agent-based model of a typical regional power system that incorporates the features of specific plant types and their cooling systems that are dependent on adequate water supplies at appropriate temperatures to support full power operation. The effects of capacity expansion plans, power demand growth, climate change, and extreme events are analyzed through different scenarios designed to illustrate the utility of such a model and show where it can aid in mid- and long-term planning.

© 2018 Elsevier B.V. All rights reserved.

1. Introduction

Electric power and water provide vital services to society. As such they are designated by the U.S. government as critical infrastructure *lifeline* sectors. Nearly all the remaining U.S. critical infrastructure sectors depend on power and water to produce their goods and services [1]. Both electric power and water and wastewater systems draw upon natural water resources to enable the provision of their lifeline services. This common source—natural water resources—creates an interdependency between power and water critical infrastructure systems. When natural water resources become scarce due to drought, disasters, or mismanagement, electric power and water and wastewater systems may compete for use of that scarce resource. In a worst-case scenario, the scarcity of natural water resources could result in electric power and water shortages that adversely affect the health and economic wellbeing of a region.

The challenge of interdependency planning is deepened by the fact that different regions rely on different combinations of fuel for energy production, have different supply and

* Corresponding author.
E-mail address: jrthompson@mitre.org (J.R. Thompson).

[1] Approved for Public Release; Distribution Unlimited. Case Number 18-0964 ©2018 The MITRE Corporation. ALL RIGHTS RESERVED.

https://doi.org/10.1016/j.ijcip.2018.12.002
1874-5482/© 2018 Elsevier B.V. All rights reserved.

demand profiles, have different amounts of water availability, and have different current and projected climates [2]. To reduce the possibility of future power and water shortages, regional and local power and water authorities should account for their mutual dependence on the same regional natural water resource supply. However, due to organizational barriers, differences in planning cycles, differences in geographic jurisdiction, and lack of joint planning tools, power and water authorities often do not engage in such joint planning.

All of this suggests a growing need for models and simulations that allow decision-makers to gain insights into the interactions and feedback structures of power and water on a local, regional, national, and global scale. Agent-based modeling (ABM) is a paradigm for analysis that is ideal for capturing complex effects and heterogeneity exhibited by agents in a system. In this paper we present the agent-based Interdependent Critical Infrastructure Model (ICIM), which is intended to facilitate joint long-term planning and thereby help authorities to avoid future power and water shortfalls.

This effort seeks to extend infrastructure models to a regional scale in a manner that can be employed by both national and regional long-term planners. By applying ICIM to a specific, constrained geographic region, we can identify potential vulnerabilities and failure points in power-water interdependencies. The characteristics of individual power sources are captured in the agent descriptions. Similarly, the dispatch algorithms used by the Electric Reliability Council of Texas (ERCOT) are approximated and encapsulated, as are the decision processes for determining water restrictions and usage outlined by the Lower Colorado River Authority (LCRA).

A key differentiator of ICIM is its focus on long-term planning. Existing, functional power-water planning models often focus on short-term, event based interdependencies (e.g., [3–5]). ICIM provides a capability that incorporates multiple time scales, starting at a granular 15-minute power demand level, and building up to a multi-year time frame that can support the analysis of the impact of extended periods of drought. By integrating the different decision-making time scales of power and water, ICIM can perform analysis and evaluation across several areas identified by the Department of Homeland Security as lifeline critical infrastructures including electric power, water, nuclear systems, dams, agriculture, and other critical elements and services in a regional economy (e.g., [6] and [7]).

In the sections that follow, we introduce ICIM as a tool template that can facilitate joint long-term planning for critical infrastructures. In Section 2 we review some of the federal and local policies that impact power and water management and discuss the modeling literature pertinent to the ICIM design. Section 3 presents the technical details of ICIM, including the construction of input variables. Section 4 describes the experiments designed to illustrate the utility of ICIM. The results of each experiment are presented in subsections immediately following each scenario description. Note that Thompson et al. [8] presented a preliminary abridged version of the model described in Section 3 and some of the results in Section 4. We conclude in Section 5 with a summary and discussion of future work.

2. Background and literature review

In this section we review the federal and local policies that impact power and water management and discuss how long-term capacity plans are currently conducted. We also review different studies that can be used as data sources in capacity planning and discuss the modeling literature pertinent to the ICIM design.

2.1. Policy

The U.S. government's National Infrastructure Protection Plan-2013, prepared as directed by Presidential Policy Directive 21 (PPD-21)[9], recognizes the interconnectedness and interdependency within the nation's critical infrastructure and states that "the extent to which infrastructure is interconnected shapes the environment for critical infrastructure security and resilience." Each of the individual critical infrastructure sectors takes up the issue of interdependency with other sectors within its sector-specific plan. The Department of Energy, as the Energy Sector-Specific Agency, acknowledges that "a comprehensive understanding of such interdependencies enables the sector to mitigate potential vulnerabilities and helps ensure that the nation's economy continues to delivery goods and services during extraordinary events" [10]. Similarly, the Environmental Protection Agency (EPA), as the Water Sector-Specific Agency, describes its interdependency with the Energy Sector as the *primary* interdependency [11].

2.2. Long-term capacity planning

Long-term plans, generally with a time horizon of 25 years or more, involve a large number of uncertainties explored through "what-if" scenarios. Such plans undergo periodic revision as uncertainties are clarified. The long-term perspective is necessary in view of the extended period for the acquisition and approval of plant sites and the wide-ranging socio-economic trends that affect housing, industry, and transportation with attendant power and fuel demands. Specific capacity expansion investment plans then encompass a shorter time horizon—5 to 15 years—to begin addressing the challenges outlined in long-term plans [12].

Partial equilibrium energy system models of note that have been applied to long-term policy planning and capacity expansion at the national level with regional content include total energy system models (electric and non-electric sectors) such as EIA-NEMS [13], EPA-MARKAL [14], and a highly regional electric system model, NREL ReEDS [15]. These models employ mathematical programming to develop constrained optimal solutions, usually over a 30-year time horizon, though in some cases they are applied to greenhouse gas mitigation scenarios spanning 30-100 years. They involve numerous dynamic constraints; however, the optimization is generally based on projected costs of alternative fuels and plant types, again introducing major future uncertainties addressed through scenario analysis.

The use of water for power generation involves both withdrawals and consumption. Withdrawal refers to the process

where the water is passed through a steam condenser and returned to its source as heated water. Consumption is where the water is utilized for cooling and other purposes and ultimately discharged in waste streams or evaporated to the atmosphere. NREL has published coefficients for both withdrawals and consumption by various types of plants [16]. The Energy Information Administration (EIA) publishes surveys of water use and other plant characteristics [17].

2.3. ERCOT and Brattle group studies as information sources

The content of ICIM and scenarios for analysis drew upon the ERCOT and LCRA publications, along with supporting material developed by the Brattle Group. These sources facilitate a realistic demonstration environment for a model designed to be portable to other regions with differing characteristics. The information sources for this analysis of power-water interdependencies thus include other sources related to differing environments. The results and projections presented in this paper are not to be taken as independent projections for policy purposes, but rather to demonstrate the utility and significance of the particular modeling approach.

The ERCOT and LCRA service regions have experienced severe droughts and conditions that threatened power production (2011-12 drought) while maintaining critical services. The maturity of the power and water planning processes and policies in ERCOT and LCRA, and the demonstrated ability to withstand severe weather events [18], provide a strong foundation for the added capabilities of a high fidelity ABM that draws on that experience.

Rather than using explicit long-term LCRA plans, the analysis drew on capacity expansion strategies from the larger ERCOT service area outlined in a Long-Term System Assessment Report [19] supported by the Brattle Group [20]. The assessment covered the 2014-2029 period and provides a foundation for near and mid-term capacity expansion plans. Where additional data were needed for the demonstration of the ABM, factors were estimated based on general sources and may not represent ERCOT or LCRA-specific data.

The ERCOT base case projection was used as a guide for the assumptions regarding annual demand growth in the 1.0% to 1.8% range, retirement of older coal-fired plants, and new capacity including solar, wind, and natural gas combined cycle plant options for the base, challenge, and mitigation scenarios outlined in this paper. As evidence of the uncertainties in long-term power planning and policies designed to respond effectively, ERCOT published a later report [21] that portrayed significant reserve margins to the 2027 period. Rather than requiring a specific reserve margin, a new ERCOT policy is based on a “reserve target” and the use of an Operating Reserve Demand Curve (ORDC) to drive capacity investments when needed [22].

2.4. Climate projections

A major source of uncertainty in long-term power and water planning is climate change. The Intergovernmental Panel on Climate Change (IPCC) periodically assesses the scientific and socio-economic factors that lead to increased greenhouse gases in the atmosphere. Using an open process that solicits feedback from experts in the field, they publish different scenarios that consist of a table of trace gas concentrations on a global scale [23]. The trace gases are, in turn, the key input parameters for well-established physical climate models (e.g., [24–26]). The output of these physical models translates the trace gas concentrations from IPCC into water and temperature estimates across the globe.

Extensive weather modeling exists in the literature. Liang [27] developed the Variable Infiltration Capacity (VIC) model whereby daily or sub-daily inputs including precipitation, air temperature, wind speed, downward shortwave and long-wave radiation, and vapor pressure and allows for the simulation of water balances at the land surface. This land surface modeling can be coupled with streamflow routing models [28,29] and stream temperature models [30] to further determine water volume and temperature availability. The VIC model has notably been used by Vliet [31] to identify vulnerability of the electric supply to climate change.

2.5. Agent-based modeling

Agent-based models are quickly becoming a mainstay in the analysis of complex adaptive systems. Miller and Page define a complex adaptive system to be one where complete understanding of the individual components does not automatically render perfect understanding of how the whole system will behave [32]. Rinaldi et al. note that critical infrastructures are all complex adaptive systems that exhibit interdependencies [33]. They define an interdependency to be “a bidirectional relationship between two infrastructures through which the state of each infrastructure influences or is correlated to the state of the other”. They go on to say that such systems are modeled effectively by collections of interacting agents. Ouyang also recognizes critical infrastructures as complex adaptive systems and reviews a number of modeling and simulation approaches to assessing critical infrastructure, including ABMs that are employed by the U.S. National Labs and other independent researchers [34].

ABMs allow analysts to simulate individual system components as *agents* interacting in a representation of their normal operating environment to gain quantitative insights into the system as a whole. Although many ABMs are built to study social systems [35], several facets of the power grid have already been modeled using ABMs. Barton et al. extended the Sandia National Lab model known as ASPEN to include electricity systems in an attempt to show how market conditions impact the electrical power production in the U.S. economy [36]. Vesleka et al. introduced the Electric Market Complex Adaptive System Model (EMCAS) in 2002 as a tool for analyzing the rapid decentralization taking place in power markets [37]. Sun and Tesfatsion also modeled the power markets with the Agent-based Model of Electricity Systems (AMES) that attempts to capture the strategic actions of traders competing to buy and sell electric power [38]. Water management has also been modeled using ABMs. Becu et al. for example, modeled the small catchment management in Thailand using a multi-agent simulation to represent the relevant stakeholders. Galánlan et al. used an ABM to demonstrate the influence of urban dynamics and socio-geographic effects on metropolitan water

management [39]. Although ABMs are widely recognized as being well-suited for modeling critical infrastructure, they do have a few weaknesses. Ouyang points out that the quality of an ABM depends on the assumptions made about how agents will behave under certain circumstances and whether or not sufficient data exists to calibrate the model correctly [34]. Rai and Douglas also point out that sufficient data and the lack of careful validation are weaknesses of the ABMs they reviewed [40].

When power and water critical infrastructures are treated as components of one system — and their respective components are looked at individually — they create a complex interdependent system that is adapting in time to provide vital services to the community. As the environment that affects the delivery of these vital services changes (demand, temperature, water availability, federal policies, etc.) these components react in different ways. Agent-based modeling provides an ideal tool for capturing these reactions and the complex system level behavior created by their interdependency.

3. Model design

The policies discussed in the previous section create a clear federal mandate from the national level on down to the individual sector level to consider sector interdependencies in security and resilience planning and implementation. The ICIM tool described in this section is intended to support and enable this federal mandate.

3.1. *The Interdependent Critical Infrastructure Model (ICIM)*

ICIM consists of power plant agents of different fossil fuel types, a hydro-electric dam agent, a wind farm agent, a solar farm agent, a centralized agent that manages the dispatch of power, water objects that are representative of the reservoirs that provide cooling water for the power plants, and a water management agent that releases water based on environmental conditions. The inputs that drive the agents' decisions are the demand for power, the available quantity of water, the surface temperature of cooling water, and the current wind speed that fuels the wind farm agent. Each of these inputs are data-driven from empirical data sets collected in the LCRA region of Texas. Fig. 1 illustrates these different components and their relationships to one another. One of the advantages of using agent-based models is the ability to incorporate heterogeneous agents. In this case, heterogeneity in power plants is defined primarily by fuel type, relative cost of fuel, cooling technology, and nameplate capacity. For each power plant agent, we designed a customized algorithm that represents the decision-making process a typical plant of that fuel type would employ to determine their available capacity at a given 15-minute interval. The constraints on the decision process include the current state of the generators, the inlet temperature and availability of their cooling water, emissions regulations, and the amount of power requested by the Independent System Operator (ISO). These algorithms are complex in nature as illustrated in Fig. 2 and are executed iteratively within the model at each time-step representing a 15-minute interval.

3.2. *The independent system operator agent*

The dispatch of electrical power is a complex process unto itself, even without the consideration of water availability [41]. The function of the ICIM ISO Agent is to administer the dispatch process in a close approximation to how actual ISOs dispatch power. Due to the physical properties of electricity and the various constraints (such as ramp rates, water temp, and nameplate capacities) on generators, the process of providing electrical power requires around-the-clock management. In the U.S., regional transmission organizations or ISOs manage this process on a real-time basis. Because electrical power cannot be adequately stored in the quantities required to meet demand, the ISO dispatches power to exactly meet demand as close to real time as possible. ERCOT is the ISO that includes the LCRA region of Texas and they recalculate the necessary power dispatch at each generator every 15 min. The calculation relies on the direct current (DC) approximation to the alternating current (AC) power flow equations [41], which accounts for the individual characteristics of each power plant, the physical properties of the transmission grid, and Kirchhoff's laws for the conservation of power in a circuit. ICIM approximates this process with the ISO agent. At each time step, the ISO receives a demand signal for power and a signal from the wind, hydro, and solar agents as to how much power they are able to produce based on environmental conditions. The power plant agents also submit their capabilities to produce power based on technical and environmental constraints. The ISO then dispatches the most economic mix of power plants to meet the demand in the next 15-minute interval that is not met by the renewable power sources. This optimal dispatch takes into account a forecast for demand one period beyond the current period. The forecast improves the economic dispatch by signaling less expensive plants to start ramping up their power outputs to meet an upcoming increase or more expensive plants to ramp down in the case of an upcoming decrease in demand. For simplification purposes, ICIM does not consider transmission constraints when dispatching power. The full formulation of the optimal dispatch process solved by the ISO agent at each 15-minute time step is:

$$\min: \sum_i C_i p_i + M \sum_i y_i + C_E E \qquad \text{//Minimize cost}$$

s.t.:

$$\sum_i p_i + E = D_p \qquad \text{//Meet demand}$$

$$p_i \le p_i^{\max} \qquad \text{//Plant capacity}$$

$$|p_i - p_{i,t-1}| \le rs_i \Delta t \qquad \text{//Ramp rate}$$

$$|E| \le 200 \qquad \text{//Limit import export}$$

$$y_i \ge 0 \qquad \text{//Min threshold variable}$$

$$y_i \ge p_i^{\min} - p_i \qquad \text{//Encourage above min}$$

where C_i is cost per megawatt (MW) produced at plant i; p_i is the amount of power dispatched by plant i in MW; E is the amount of power bought from or sold to the rest of the power

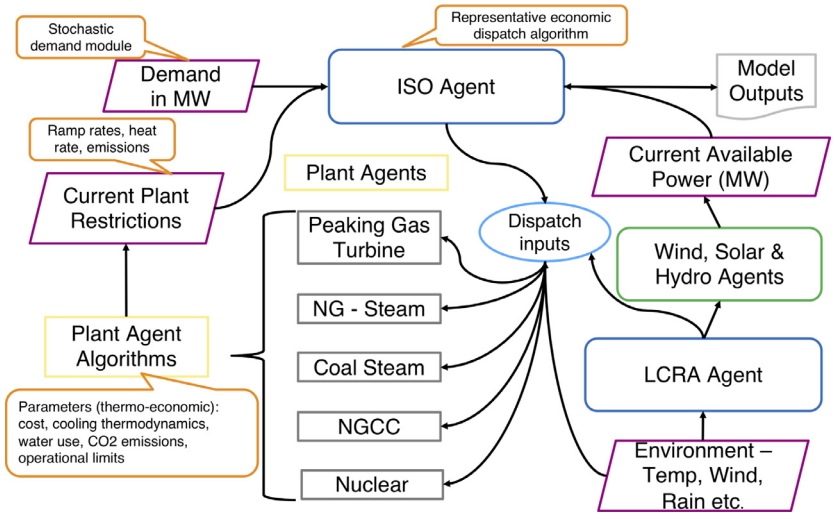

Fig. 1 – Agent-based model structure.

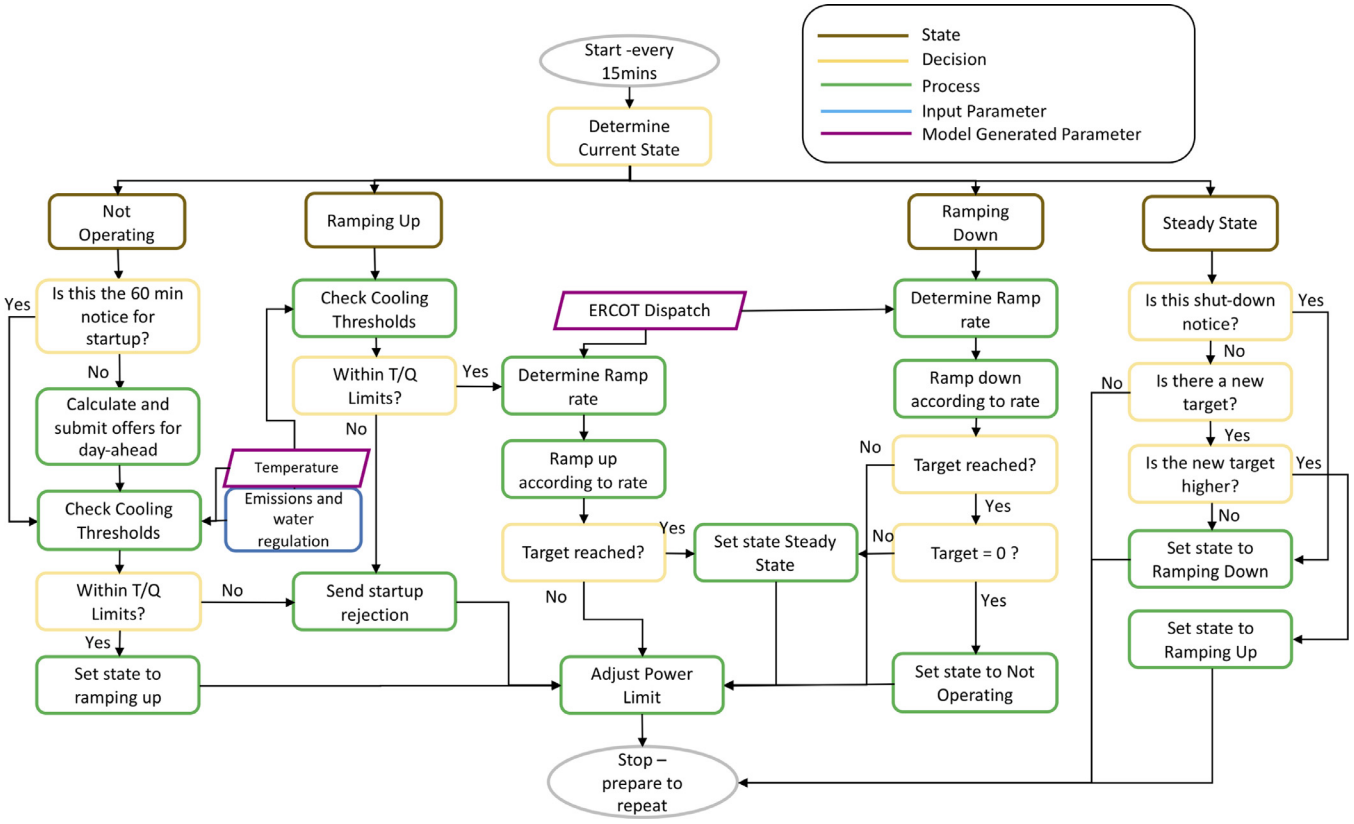

Fig. 2 – Decision algorithm for a combined-cycle plant.

grid; C_E is the cost of power E; y_i is the penalty scale for operating plant i below its recommended minimum; rs_i is the ramp speed in MW per min of plant i; Δt is the amount of time since last solving the optimal dispatch; and D_p is the total amount of power demanded at the current time. The last two constraints encourage each plant to stay above the minimum threshold, but allows them to dip below, if necessary, to meet demand exactly. These transgressions are monitored for model comparison and validation. When there is no feasible solution because the plants cannot supply enough power, every plant is increased by the largest amount possible. The reverse is true if the plants over supply power. The changes for both conditions are restricted by minimum and maximum available capacity.

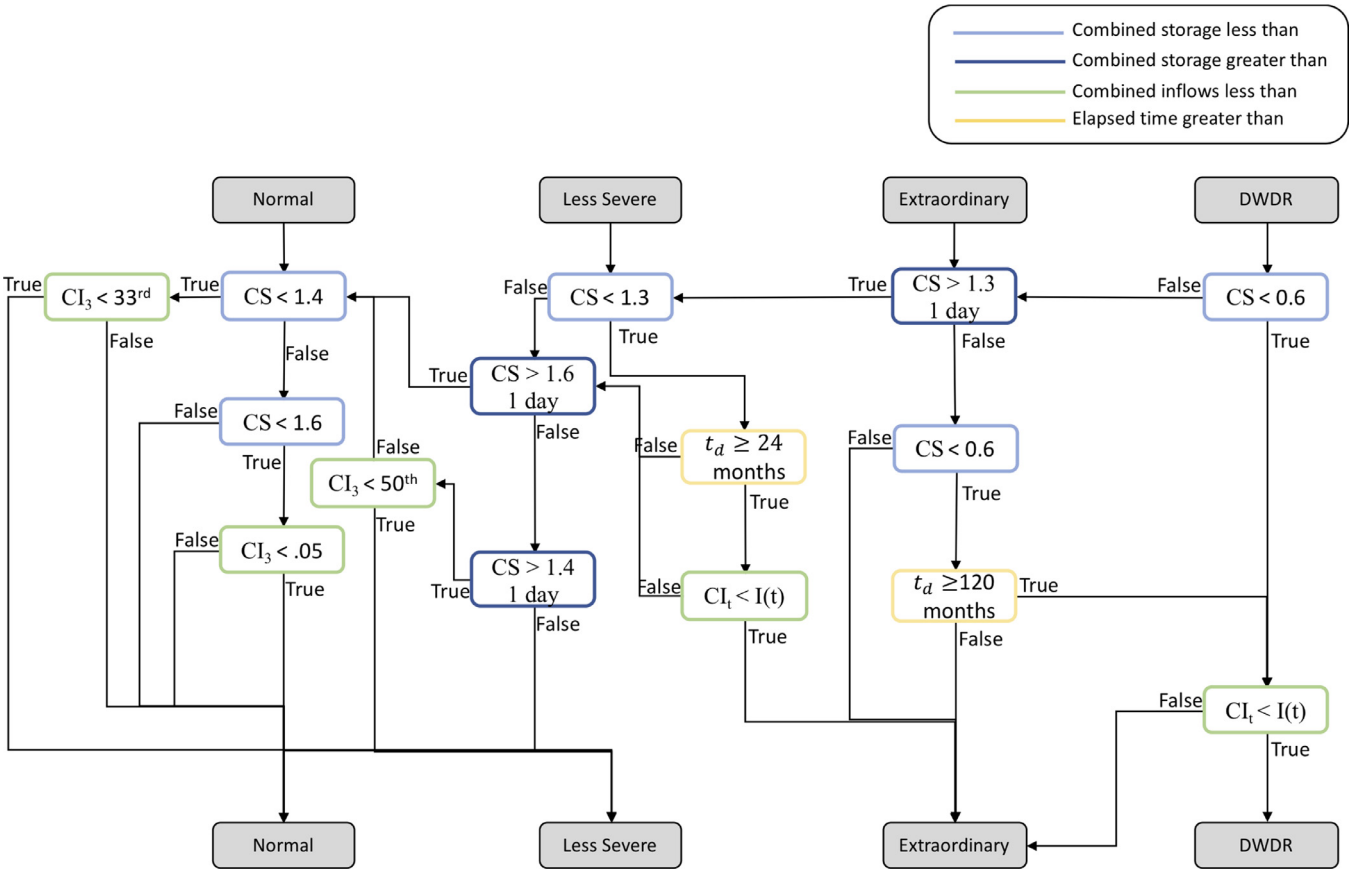

Fig. 3 – The decision process used by the LCRA board of directors to determine drought status.

3.3. *The water management agent (LCRA)*

To set up the rules that control the simulated water system, ICIM uses the drought contingency plans described in the LCRA Water Management Plan (WMP) submitted in 2015 [42]. The WMP contains information about the specific trigger levels and conditions that are used to determine the amount of Interruptible Stored Water (ISW) in lakes Buchanan and Travis that is available for agricultural and environmental needs downstream. The water management agent, called LCRA, tracks the ISW and properly updates the water system throughout the simulation and measures any impact on agriculture that results in each scenario. The WMP was created with the goal of maintaining Firm Water demands through conditions like those of the historic 1950s Drought of Record (DOR) by curtailing the ISW.

Fig. 3 shows the decision process that the LCRA Board of Directors uses to determine whether the water system status is: Normal, Less Severe Drought, Extraordinary Drought, or Drought Worse than Drought of Record (DWDR). Combined Storage (CS) and Cumulative Inflow over t months (CI_t) are measured in million acre-feet. Drought duration (t_d) is measured in months. The decision blocks with 33^{rd} and 50th refer to the 33^{rd} and 50th percentile inflows within the U.S. Geologic Survey database. The decision blocks that look at CS with the "one day" caveat ask whether the CS was larger than that number for at least one day in the previous period. Lastly the Envelope Curve $I(t) = 846,940e^{0.0184m}$ is used in cases of extended drought for comparing cumulative inflows. They evaluate status on March 1 for Crop Season One and July 1 for Crop Season Two. The water available for release as a result of the March 1 evaluation is released during March, April, May, June, and July. The July 1 evaluation dictates available release for August, September, and October. In addition, any available ISW not used in Crop Season One can be used during Crop Season Two. Table 1 shows the cutoffs and allotments for both crop seasons by drought status. No ISW is available in Extraordinary Drought or DWDR. Lastly, there is an "anytime cutoff" wherein all ISW is ceased if CS drops below 0.9 million acre-feet (MAF) in Normal status or 0.95 MAF in Less Severe Drought.

It should be noted that water management plans will differ from one region to the next due to differences in raw water sources, population factors, and other environmental factors including local and national policies. ICIM provides a framework for a representative water management agent based on LCRA's published water management plan, but can be easily updated with any regional plan where priorities and thresholds may be different.

3.4. *Input analysis and model calibration*

The major inputs that drive ICIM are the water surface temperature, wind speeds, solar availability, and the demand for

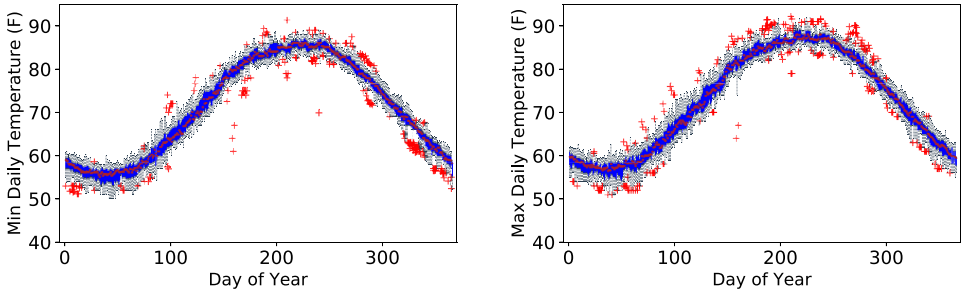

(a)Minimum Daily Temp. (b)Maximum Daily Temp

Fig. 4 – Lake Travis surface temperature profile.

Table 1 – Total interruptible stored water available for agricultural operations under normal water status and less severe drought status.

Normal water status			
First crop season		Second crop season	
Combined storage on March 1 (million acre-feet)	Interruptible stored water (acre-feet)	Combined storage on July 1	Interruptible stored water (acre-feet)
Below 1.0 MAF	0	Below 1.0 MAF	0
1.0 to 1.3 MAF	121,500 to 202,000*	1.0 to 1.55 MAF	46,000 to 59,500*
1.3 MAF or above	202,000	1.55 MAF or above	76,500
Less severe drought status			
Below 1.1 MAF	0	Below 1.1 MAF	0
1.1 to 1.199 MAF	100,000	1.1 to 1.399 MAF	46,000
1.2 to 1.299 MAF	115,000	1.4 to 1.599 MAF	55,000
1.3 to 1.399 MAF	130,000		
1.4 to 1.499 MAF	145,000		
1.5 to 1.599 MAF	155,000		

* For combined storage within the specified ranges, the interruptible stored water supply available follows a linear scale between the values shown.

electrical power. Using 20 years of daily temperature data for Lake Travis, we created an annual temperature profile for minimum, average, and maximum daily temperatures. Other LCRA region lakes were observed with less granularity and for a shorter time period so Lake Travis was used as the baseline. Lakes with sufficient data are compared to the Lake Travis temperature profile and adjusted accordingly. Some of the lakes in the region have no public temperature data, so we assumed they follow the same distribution as Lake Travis. To simulate the daily temperature profile for each lake, we randomly generated a minimum and maximum daily temperature from two separate Gaussian distributions defined by the Lake Travis temperature profile and accounted for any shifts necessary to adjust to the specific lake. We then fitted a sinusoid that places the minimum temperature at 2:00 a.m. and the maximum temperature at 2:00 p.m. That is,

$$min = \bar{x} - \left|N\left(\mu_L, \sigma_L^2\right)\right|$$

$$max = \bar{x} + \left|N\left(\mu_H, \sigma_H^2\right)\right|$$

$$f(t) = \frac{max - min}{2} \sin\left(\frac{2\pi t}{1440} - \frac{\pi}{2}\right) + \frac{max + min}{2} \quad (1)$$

where $\bar{x}$ is the average daily temperature, μ_L and σ_L^2 are the mean and variance of the daily low temperature, μ_H and σ_H^2 are the mean and variance of the daily high temperature, and $f(t)$ gives the temperature as a function of time t. The temperatures were updated hourly within the model.

The wind speed input is purely data-driven. We employed hourly wind speed data for one year at both the Pecos and Corpus Christie wind farms. The focus of our model is the interdependencies between power plants with intense water needs and water management that supplies both power plants and the population. The main contribution of wind power is to supplement power supply when possible with little direct connection to water. Thus, for our purpose, a data-driven input is sufficient to represent wind and can be easily adjusted to accommodate future forecasts.

For solar-thermal power we assumed availability between the hours of 6:00 a.m. and 6:00 p.m. following a quadratic curve that peaks at 12:00 p.m. We did not assume a stochastic component for solar power.

To determine the demand for power input, we used ERCOT's public data that recorded the power supplied every 15 min for the year 2015 broken down by region across ERCOT's coverage area, including LCRA. The demand for power is driven by human activity, which is periodic in nature. Societies generally follow similar schedules of working eight to ten hour days, five days a week during the daylight hours.

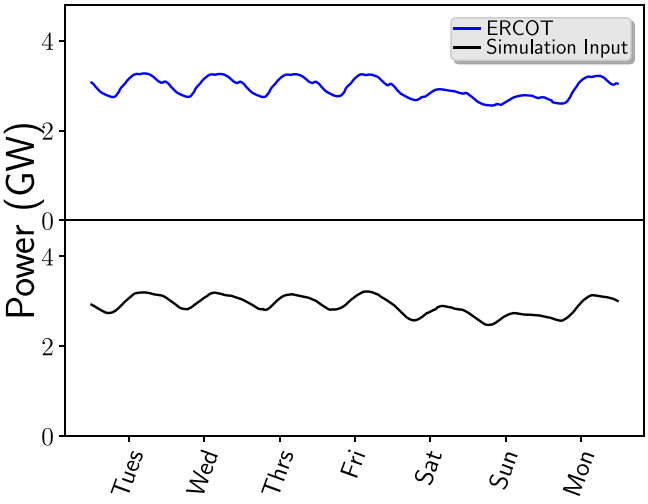

Fig. 5 – Seven days of ERCOT Data (Blue, Top) and ICIM Input (Black, Bottom).

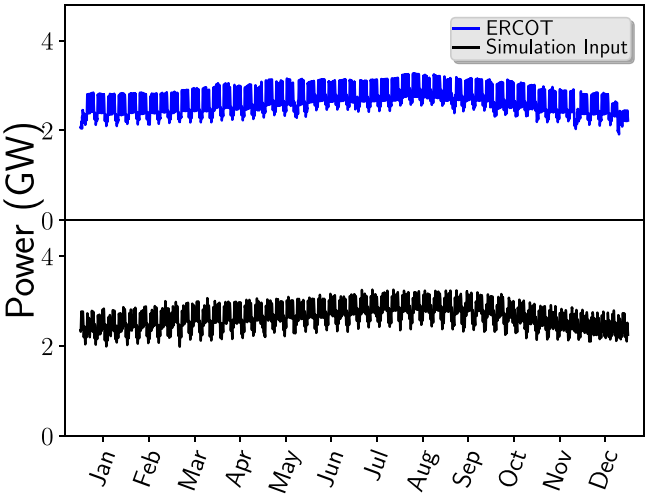

Fig. 6 – The year 2015 of ERCOT data (Blue, Top) and ICIM input (Black, Bottom).

These patterns are directly reflected in the demand for power and are influenced by the day's temperature cycle. As a result, the time series of power demanded is well-approximated by a trigonometric polynomial that accounts for daily, weekly, and seasonal frequencies of a given region. Using the 2015 dataset from ERCOT, we employed Fourier analysis to extract the 10 most resonate frequencies and regressed the data on the resulting polynomial. The residuals from the regression exhibited an auto-correlation structure that we were able to isolate using an auto-regressive moving average (ARMA) process. The final set of residuals fit a Student's t-distribution with 2.21 degrees of freedom and passed the Box-Ljung portmanteau test for independence [43]. The ICIM input function for power demand, $P_t = \sum_i p_i$ at time t, employed the 10 frequencies, the ARMA(2, 2) fit, and a t-distributed random variable as follows:

$$P_t = c + \sum_{j=1}^{10} a_j \sin(2\pi\omega_j t) + \sum_{j=1}^{10} b_j \cos(2\pi\omega_j t) + \sum_{k=1}^{2} \phi_k \varepsilon_{t-k} + \sum_{k=1}^{2} \psi_k \varepsilon_{t-k} + \varepsilon_t \quad (2)$$

where ε_t is t-distributed with 2.21 degrees of freedom and c is a constant that can be adjusted to shift the demand curve up or down.

In order to verify that our model inputs were correctly calibrated to the empirical data, we generated seven days from the power demand function and compared them with seven days from the same time frame in the original ERCOT data in Fig. 5. We also compared the entire baseline year of 2015 against a year from the simulation input function in Fig. 6. The simulation time series is shown in black while the original ERCOT data is depicted in blue.

We also compared the Fourier transform from the ERCOT 2015 dataset with that of the simulation input as shown in Fig. 7. Once the model inputs were confirmed to be good statistical representations of the empirical data, we adjusted the various model parameters to similarly calibrate model outputs to the EIA data available for the LCRA region. The power plants represented by agents in ICIM are specifically modeled on:

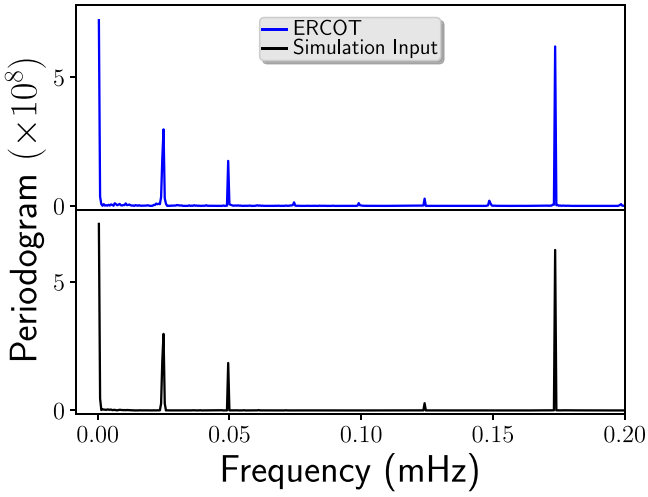

Fig. 7 – Spectral analysis of ERCOT demand compared to ICIM input function.

- The South Texas Nuclear Project
- Sandy Creek Energy Station
- Fayette Power Project
- Lost Pines Power Project
- Thomas C. Ferguson Power Plant
- Winchester power park
- Sim Gideon power plant

The combined annual production of the plants above was reported as 38.08 million megawatt-hours (MWh) in 2015. Recall from Eq. (2) that the model inputs are calibrated to the resonant frequencies and auto-regressive characteristics of the data, whereas the 38.08 million MWh represents the sum total

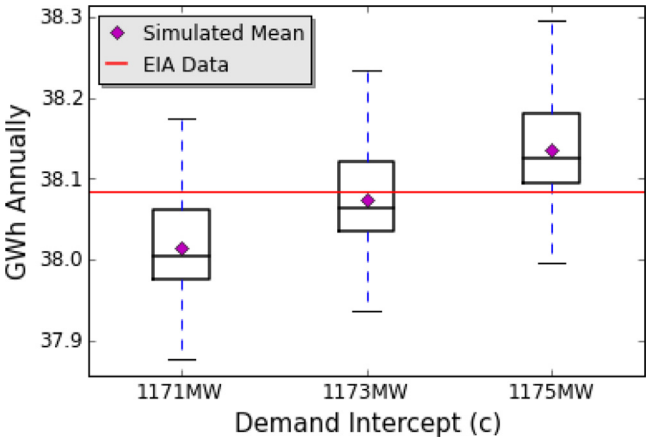

Fig. 8 – Calibration of total production to 2015 (1.5 x IQR method).

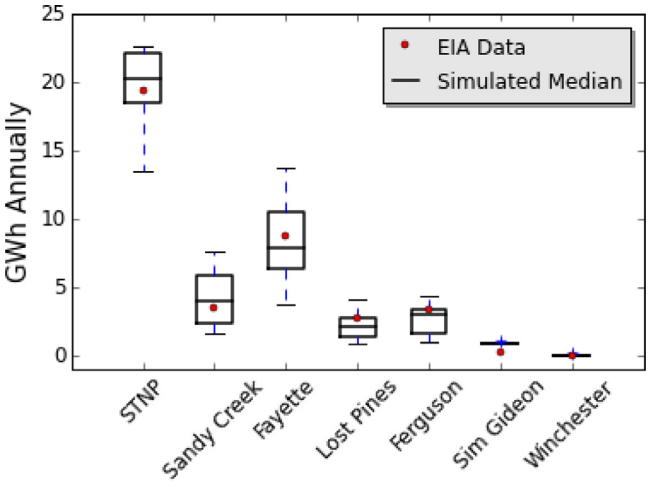

Fig. 9 – Calibration of individual plants to 2015 production (1.5 x IQR method).

of annual production. That is, the integration of the 15-minute power demand curve over the entire year should yield 38.08 million MWh. To calibrate to this value, we held all parameters within Eq. (2) constant except for the intercept parameter c. By adjusting c up or down we can alter the annual production while maintaining the statistical characteristics evident in the data (see Fig. 8). This constitutes an assumption that the shape and volatility of the demand curve is scale-invariant within a certain range of total production. In general, this assumption may not be true as certain plants are often relied upon for either base load or peak load. Thus, a base load plant may have a fairly constant production profile, while a peak load plant may have a more volatile demand profile. However, the mix of plants included in our model are diverse enough that we believe this assumption is reasonable. Note that all box-whisker plots in this analysis were constructed using the standard 1.5 times the inter-quartile range (1.5 × IQR) method with outliers indicated as crosses beyond the whiskers. The bar inside the box is the median and the arithmetic mean is marked by a diamond-shaped point.

In an effort to quantitatively reinforce the validity of our calibration we also calibrated the individual plant production in the model to closely match the individual plant production in the EIA data. As previously mentioned, the model does not include the transmission grid. Although the power demand curve is relatively stationary in the frequency domain, the price of power exhibits heavy tails and volatility clustering that is likely due to the influence of the transmission grid. As the demand for power increases, the transmission lines approach their maximum capacity thresholds. In response, the ISOs must dispatch more expensive power to avoid overloading transmission lines. The additional cost of the more expensive generators is passed on to the consumer through what is known as transmission congestion costs. These costs can vary significantly as the ISO constantly adjusts to the stochastic demand. Ultimately, it is the cost of both producing power and transmitting it to the desired location that drives individual plant production. We therefore adjusted the relative cost of the generators in our model to calibrate their annual production to the historical data. At each potential parameter setting we performed 30 replications of the simulation and chose the setting where the confidence intervals of those replications most closely matched the historical data point. The final calibration resulted in the matches shown in Fig. 9.

4. Experiments and results

To illustrate the utility of ICIM we designed six experiments that are predicated on the 2015 baseline calibration. That is, control variables were set to the 2015 configuration or extrapolated from those settings according to a given empirical source for future projections. The first experiment simply incorporates the ERCOT Long-term System Assessment projections for capacity expansion and demand growth out to 2030. Each of the five subsequent experiments compares the long-term capacity expansion plan under various challenge scenarios that could manifest in 2030. These are the IPCC A2 and Accelerated A2 scenarios, a temperature regulation scenario, a high economic growth scenario, an extended drought scenario, and a more severe lake loss scenario.

The results of each experiment are best viewed in terms of power produced in each 15-minute interval compared to the *available* capacity in that interval. Recall that *installed* capacity is a constant value equal to the sum of nameplate capacities of the contributing generators. In contrast, *available* capacity is a dynamic property that varies with environmental conditions and the attributes of each generator. The difference in these two values is accentuated in wind and solar power sources since their installed capacity may be hundreds of megawatts, but their available capacity is dependent on the wind blowing or the sun shining. ICIM does not model the transmission grid or cascading failures. The concepts of black-outs, brown-outs, or power shortages are captured as unmet demand. In general, the ISO may be able to import power from other regions, so that unmet demand does not result in a power shortage. Also note that costs are included in ICIM only as relative

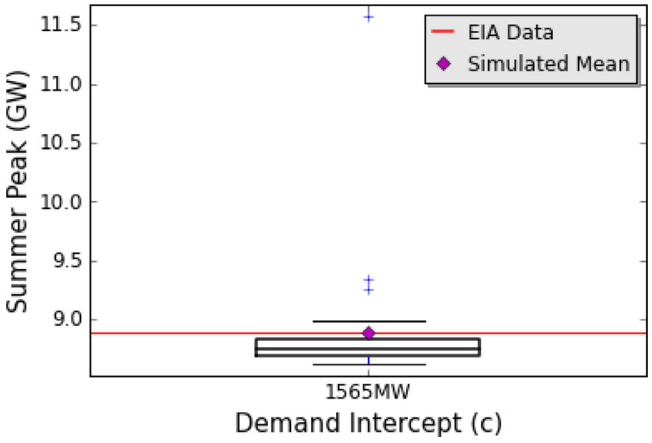

Fig. 10 – Calibration to forecast peak demand in 2030 (1.5 x IQR method).

values to ensure that historically more expensive fuel types are dispatched after historically cheaper fuel types.

In the analyses that follow we focus on unmet demand, cost, and relative adequacy of a given plan under each scenario. However, ICIM produces a number of metrics that are important to decision-makers. These include greenhouse gas emission in parts per million, lake level for each lake over time, volume of water outflow over time, the total volume of water storage over time, the surface temperature of each lake over time, and the plant level power dispatched for each plant in each 15-minute interval.

4.1. *2030 baseline scenario*

4.1.1. *Scenario description*

Given that ICIM successfully replicated the aggregate power production by plant in 2015, we incorporated the relevant 2030 projections from the Long-term System Assessment for the ERCOT Region [19]. The first step was to determine the future power demand profile. The ERCOT report incorporated six different forecasts that ranged from more energy efficient systems to a high degree of economic growth. The current trend of economic growth was approximately in the middle of these forecasts at 1.3% growth annually. Recall that the ICIM demand function from Eq. (2) incorporates the cyclic nature of power demand and is calibrated to represent only the seven power plants included in the model using the intercept parameter *c*. The 1.3% projection is an extrapolation of peak demand for all of ERCOT. Thus, we ran 30 replications of the ICIM power demand function for 2015 and took the average maximum observed to establish the 2015 peak demand for the subset of LCRA plants in ICIM. The 2030 baseline scenario demand function was then calibrated to represent 15 years of 1.3% growth annually, again by running 30 replications with a mean that closely matched the point estimate of anticipated growth. The results of this calibration are shown in Fig. 10.

The future peak demand is a critical value because installed capacity and reserve margins are calculated as functions of this estimate. ERCOT is projecting not only an increase in installed capacity, but changes to the ratio of fuel types contributing to the installed capacity in 2030. To capture this in ICIM we calibrated the nameplate capacity of plants corresponding to the particular fuel type to either increase or decrease according to the projected percent contribution to total capacity. ERCOT revised their reserve margin requirements in the 2017 Capacity Demand Reserve report [44] to 9.6% reserve margin in 2027 down from 12.77% in the 2014 report. ICIM is thus calibrated to 2030 projections by forecasting the peak demand with 1.3% growth, altering the percent change in fuel types according to projectionsx, while maintaining approximately a 10% margin between estimated peak demand and installed capacity. The balance between these points of calibration is illustrated in Tables 2–4.

Table 2 – Peak demand, reserve margin and installed capacity in 2030.

Parameter	Value
Estimated peak demand	8887 MW
Desired reserve margin	10%
Calculated installed capacity	9779 MW

Table 3 – Percent change in fuel type by 2030.

Fuel type	% projected	% calibrated
Natural gas	31.7	32.9
Nuclear	28.5	27.7
Coal steam	23.8	23.3
Hydro	3.3	3.0
Solar	7.8	8.2
Wind	5.0	4.9

Table 4 – Nameplate capacity of ICIM plants in 2030.

Plant	2030 Nameplate capacity (MW)
The South Texas nuclear project	2708.6
Sandy Creek energy station	900
Fayette power project	1380
Lost Pines power project	595
Thomas C. Ferguson power plant	565.6
Winchester power park	240
Sim Gideon power plant	623
Wirtz hydro-electric dam	289.5
Papalote II wind farm	200
Indian Mesa wind farm	82.5
Projected wind expansion	200
Projected Natural gas expansion	1195
Projected solar expansion	800

Last, the environmental control variables of initial combined water storage, monthly water inflows, water surface temperature, and wind speeds in the 2030 baseline scenario were held equal to their values in the 2015 calibration.

It should be noted that this calibration is meant to be *reasonable* in the context of current expansion plans. The purpose of ICIM is to provide an analysis tool that incorporates more

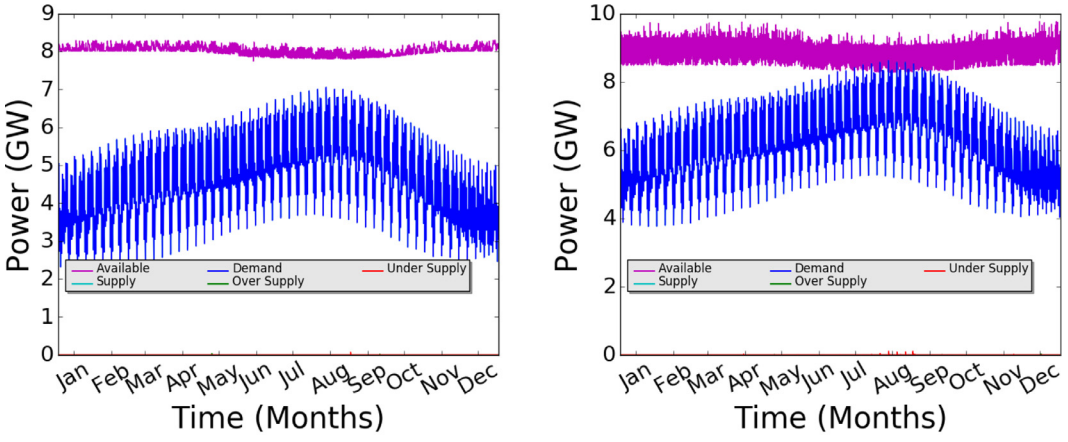

(a)The 2015 Calibration Results (b)The Baseline 2030 Results

Fig. 11 – Power demand versus available capacity.

granularity, stochasticity, and dynamic interdependency than point estimates. The parameters given in Tables 2–4 can be configured to many possible future scenarios to aid in long-term planning.

4.1.2. *Baseline 2030 results*

As described above, the baseline 2030 scenario incorporates the ERCOT Long-term Assessment parameters for reserve margin, installed capacity and projected demand growth. For each experiment, we ran a total of 30 replications each initiated with the same set of 30 random number seeds. The quantity of 30 was chosen as a balance between good sample size and our desire to limit false confidence driven by narrower confidence intervals due to their inverse relationship with sample size. By pairing replications from different scenarios that were created using the same random number seed we can employ Student's standard paired *t*-test. The null hypothesis is that the difference between the means is zero and the alternate hypothesis is that the difference is not equal to zero. When comparing the 2015 calibration settings with the baseline 2030 results, the unmet demand and amount of time in the year with less than 10% reserve margin available showed statistically significant increases. The cost per MWh showed a statistically significant decrease.

Fig. 11 shows a single replication of the 2015 calibration results (a) compared with a replication of the baseline 2030 scenario generated with the same random number seed (b). Table 5 and Figs. 12 and 13 show the statistical comparisons of three key metrics using all 30 replications of each scenario.

Note that although the system is designed to have a 10% reserve margin based on point estimates of future peak demand, the stochastic nature of both power demanded and available capacity results in a small amount of unmet demand in 2030 and intervals during the peak season where there is less than 10% margin between demand and available capacity. Note also that available capacity is significantly more volatile in 2030 as the wind, solar, and hydro generators contribute a larger percentage of power supply.

Table 5 – Statistical differences in key metrics between 2015 calibration and baseline 2030 scenarios.

Metric	Mean difference	95% confidence interval	*p*-value
Unmet Demand	4990.0 MWh	(1430.5, 8549.4)	7.638×10^{-3}
Cost	−$1.50	(−2.02, −0.97)	2.424×10^{-6}
Time less than 10%	3.7%	(3.6, 3.8)	$< 2.2 \times 10^{-16}$

4.2. *IPCC A2 and accelerated A2 scenarios*

4.2.1. *Scenario description*

Vliet et al. employed the IPCC A2 scenario to project water availability and surface temperature for the years 2031–2060 and the year 2080 [31]. The IPCC A2 scenario is representative of a more heterogeneous world characterized by self-reliance and preservation of local identities. Fertility patterns are assumed to converge slowly leading to an increased global population, while economic patterns become regionally oriented. Per capita economic growth and technological change are thus assumed to be more fragmented and slower than other possible scenarios. The general result is more greenhouse gases in the atmosphere leading to increased temperatures and decreased monthly water inflows.

We designed two climate change scenarios based on the VIC model outputs for the IPCC A2 Scenario. The first was A2 in 2030 and the second is an *accelerated* A2 that assumed the conditions of 2080 manifested much sooner in 2030. To incorporate the A2 forecasts into ICIM we adjusted the resulting temperature increases and percent reductions in water inflows into the model input parameters. In the case of temperature, recall Eq. (1) is calibrated to the minimum and maximum observed daily lake surface temperatures. The parameters μ_L and μ_H represent the average daily lows and highs respectively. To create environmental challenge scenarios in ICIM these parameters are simply adjusted by the average temper-

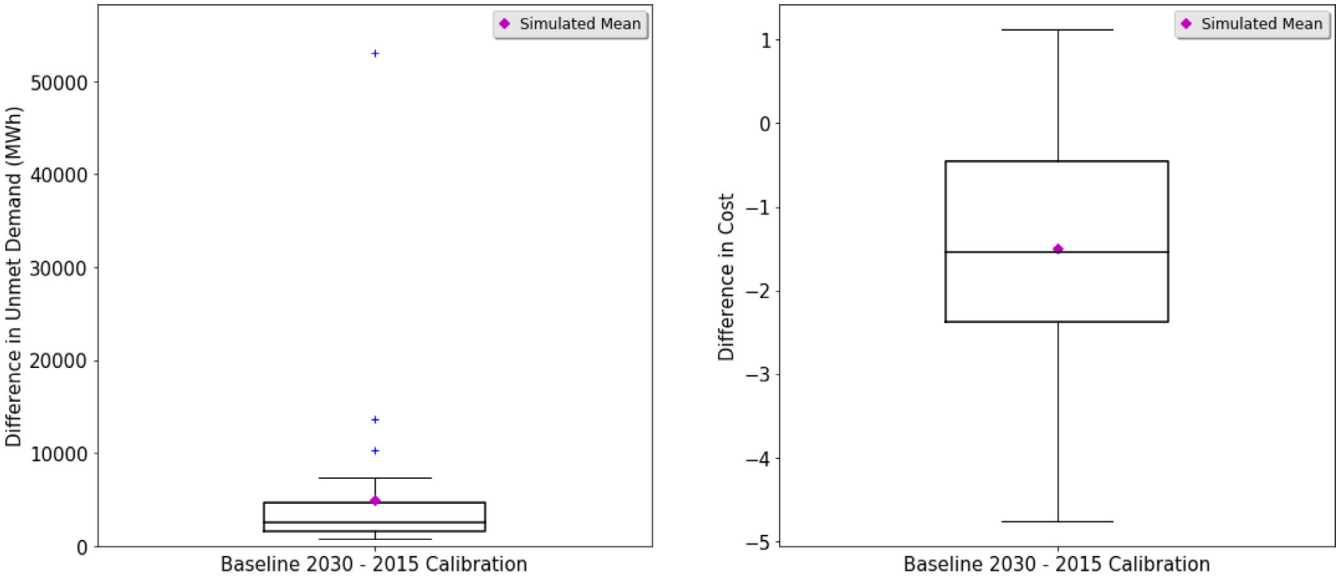

(a) Unmet Demand (b) Cost per MWh

Fig. 12 – Calibration 2015 compared to baseline 2030 ($n = 30$).

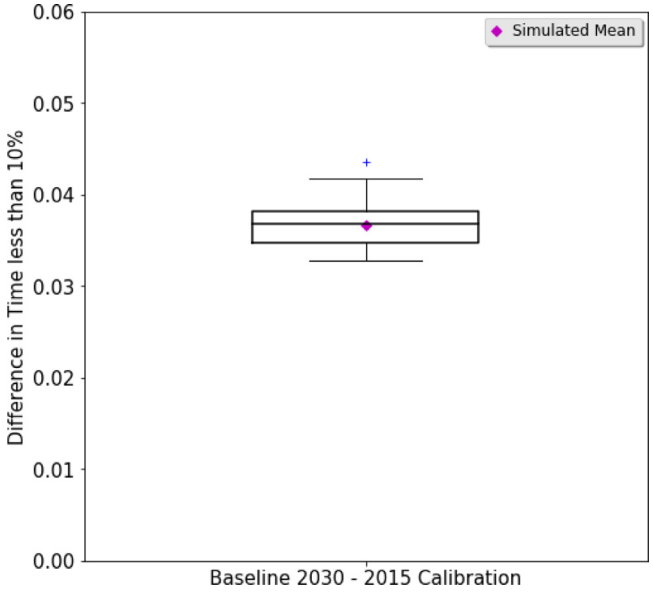

Fig. 13 – Calibration 2015 compared to baseline 2030 of time with less than 10% ($n = 30$).

Table 6 – Parameter changes for A2 challenge scenarios.

Parameter	IPCC A2 2030	Accelerated A2
$\Delta temp$	2.15 °F	4.5 °F
Annual inflow reduction	−25.0%	−50.0%
Monthly inflow	**A2 2030 % change**	**Accelerated A2 % change**
Jan	0.76	0.51
Feb	0.8	0.53
Mar	0.84	0.56
Apr	0.8	0.53
May	0.84	0.56
Jun	0.8	0.53
Jul	0.76	0.51
Aug	0.68	0.45
Sept	0.64	0.43
Oct	0.6	0.4
Nov	0.68	0.45
Dec	0.8	0.53

ature change $\Delta temp$. That is,

$$\mu_L^* = \mu_L + \Delta temp$$
$$\mu_H^* = \mu_H + \Delta temp$$
$$min = \bar{x} - \left|N\left(\mu_L^*, \sigma_L^2\right)\right|$$
$$max = \bar{x} + \left|N\left(\mu_H^*, \sigma_H^2\right)\right|$$
$$f(t) = \frac{max - min}{2} \sin\left(\frac{2\pi t}{1440} - \frac{\pi}{2}\right) + \frac{max + min}{2}$$

The monthly water inflows in ICIM are data driven. For the 2015 calibration, ICIM was populated with historical inflows from a data table. For a given challenge scenario we adjusted the historical values by the anticipated percent reduction. The final parameters used for the A2 2030 and the A2 Accelerated scenarios are shown in Table 6. The reduced inflows gradually reduces the amount of combined storage water available in the region. The net effect calculated by ICIM is shown in Fig. 14 in comparison with the baseline 2030 combined storage water over time.

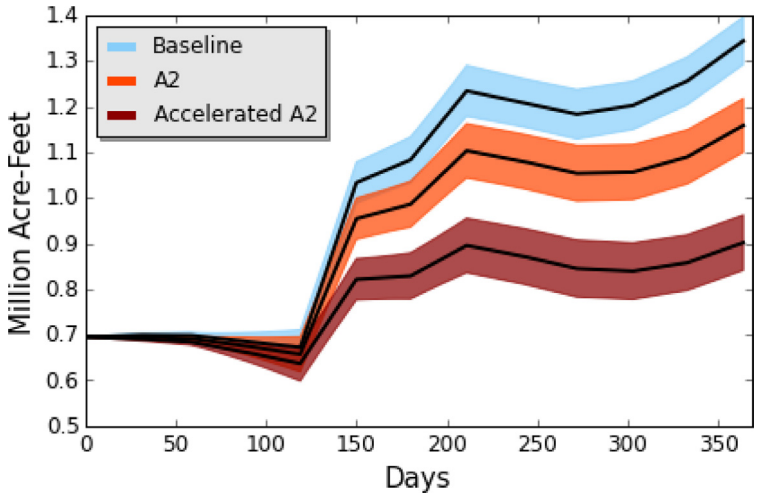

Fig. 14 – Comparison of combined storage water under baseline 2030 and IPCC A2 scenarios.

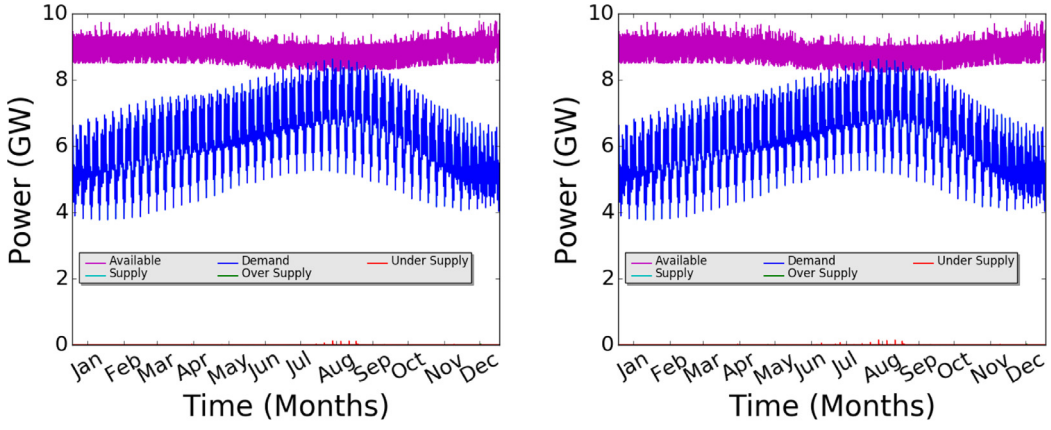

Fig. 15 – The potential impact of climate change in 2030.

Table 7 – Statistical differences in unmet demand between baseline 2030 and A2 scenarios.

Comparator	Mean difference (MWh)	95% confidence interval	*p*-value
A2 2030	834.6	(592.8, 1076.5)	9.181×10^{-8}
Accelerated A2	2096.7	(1587.3, 2606.0)	2.81×10^{-9}

Table 8 – Statistical differences in cost between baseline 2030 and A2 scenarios.

Comparator	Mean difference	95% confidence interval	*p*-value
A2 2030	\$0.03	(0.013, 0.043)	7.351×10^{-4}
Accelerated A2	\$0.05	(0.024, 0.069)	2.255×10^{-4}

Table 9 – Statistical differences in time less than 10% between baseline 2030 and A2 scenarios.

Comparator	Mean difference (%)	95% confidence interval	*p*-value
A2 2030	0.34	(0.32, 0.35)	$< 2.2 \times 10^{-16}$
Accelerated A2	0.71	(0.69, 0.74)	$< 2.2 \times 10^{-16}$

4.2.2. *IPCC A2 results*

The A2 scenarios challenge the baseline 2030 scenario with environmental conditions that could result due to climate change under the IPCC projections. Fig. 15 shows a single replication of the A2 2030 scenario and the corresponding replication of the Accelerated A2 scenario that allows 2080 conditions to manifest sooner in 2030. At this scale the plots appear similar to the 2030 baseline scenario, but there are statistically significant differences. Tables 7–9 show the mean difference between the IPCC scenarios and the baseline 2030 scenario in

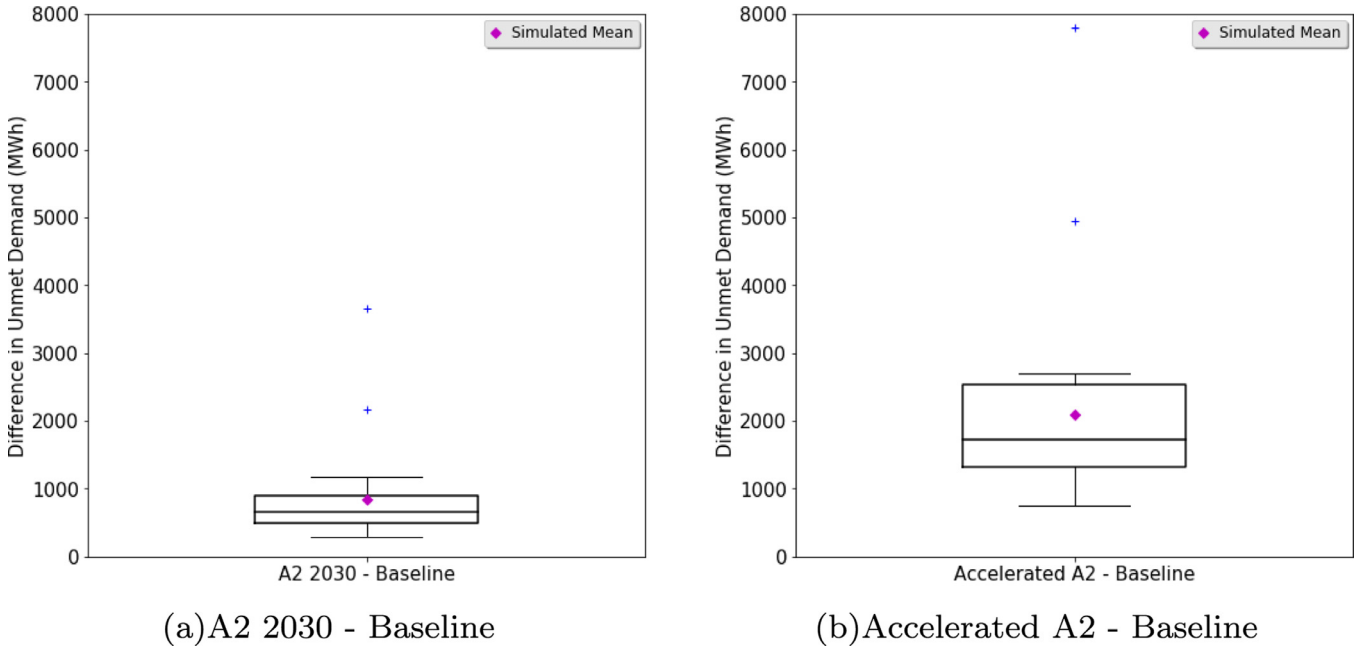

Fig. 16 – Comparison to baseline of unmet demand ($n = 30$).

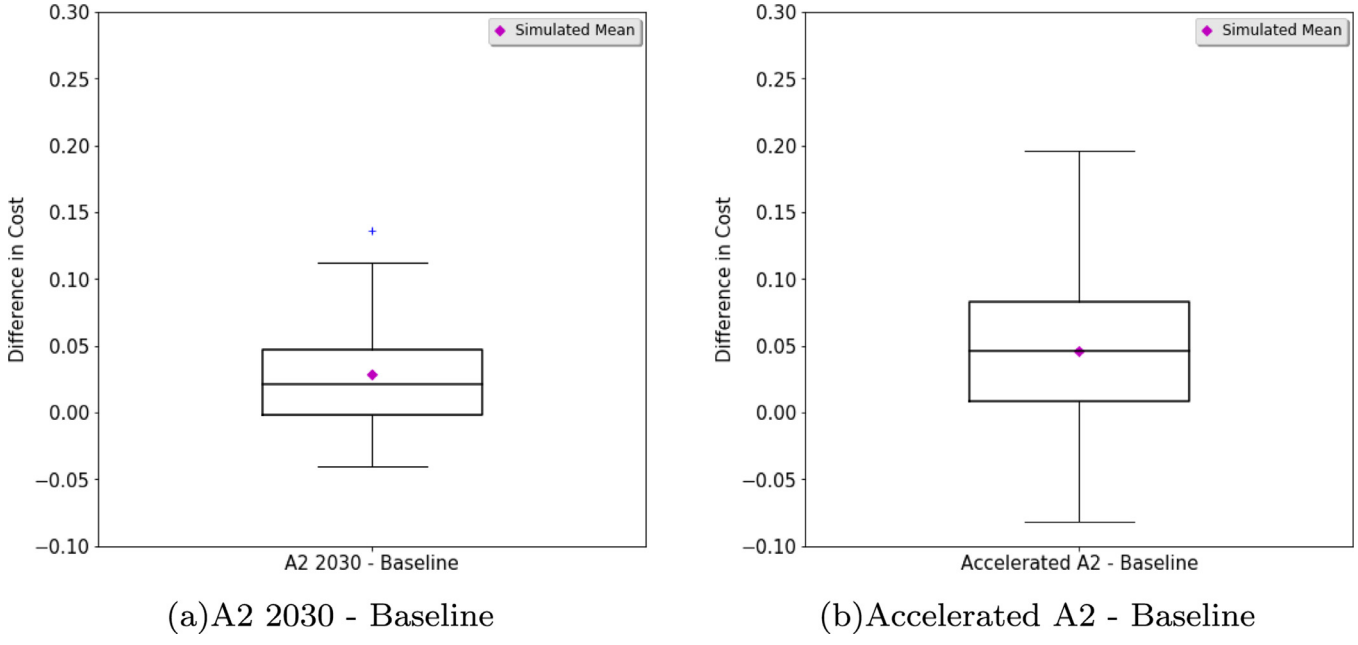

Fig. 17 – Comparison to baseline of cost per MWh ($n = 30$).

unmet demand, relative cost and percent of time when the difference between demand and available capacity was less than 10% respectively. Figs. 16–18 show the resulting box plots of these same statistics.

Note that statistical significance does not necessarily imply practical significance. A difference of one thousand megawatt-hours over an entire year may or may not be enough to change the decision of a planning committee considering a 10-year planning horizon. The purpose of ICIM is to facilitate practical decision-making by presenting the statistically significant information to decision-makers who can in turn place those values into the appropriate context.

4.3. *Temperature regulation scenario*

4.3.1. *Scenario description*

The third experiment is designed to illustrate how different environmental policies can be tested using ICIM. In this case we chose to limit the discharge temperature of electrical plant cooling water. The standard thermodynamic equations relat-

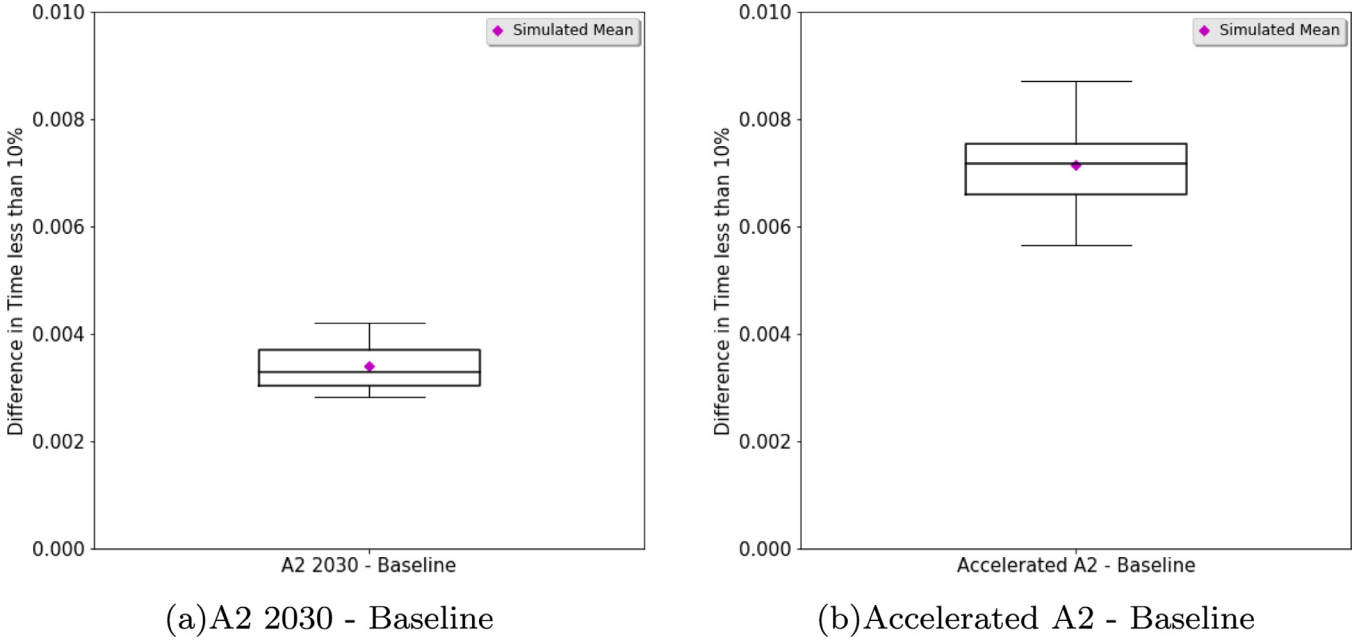

Fig. 18 – Comparison to baseline of time less than 10% ($n = 30$).

ing the production of power to the temperature change of cooling water are incorporated into ICIM. Each plant agent is able to calculate the resulting temperature change based on the number of megawatt-hours the ISO is asking them to produce and the current water surface temperature. Implementing a threshold on the water discharge temperature results in a curtailment of available capacity of each plant that varies with the ambient temperature and plant specifics, such as cooling system design and fuel type. For this scenario, ICIM was configured exactly the same as the baseline 2030 scenario except the temperature threshold was set to 115°F.

4.3.2. *Temperature regulation results*

The temperature regulation scenario was designed to illustrate how different policy proposals that impact critical infrastructure can be tested within ICIM. The scenario assumes an environmental regulation is in effect in 2030 that restricts outlet water temperatures to no more than 115°F. Fig. 19 shows the impact that such a policy would have on the 2030 baseline capacity plan.

The water temperature regulation causes a notable dip in the available capacity and unmet demand is considerably more frequent. Note also that over supply of power becomes an issue under this regulation. Plants are restricted by their ability to ramp up or down to new power output settings. This causes delays in response time when they are subjected to the stochastic nature of temperature. Table 10 shows the statistical comparison of the water temperature regulation scenario to the baseline 2030 scenario.

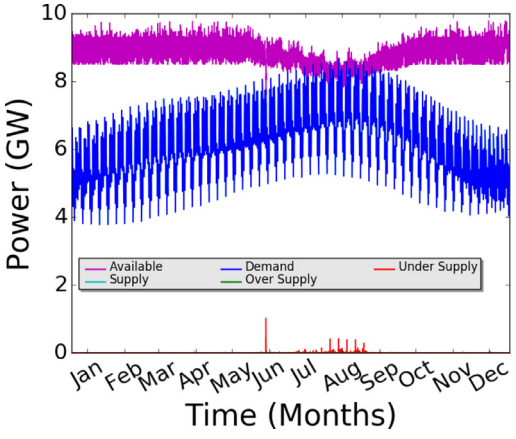

Fig. 19 – The impact of temperature regulation on the 2030 plan.

4.4. *High economic growth scenario*

4.4.1. *Scenario description*

The high economic growth scenario illustrates how long-term capacity planners might test the robustness of a particular expansion plan under different assumptions about the future. The ERCOT Long-term Assessment Report used six different forecasts of economic growth that would contribute to changes in the amount of power demanded in the region. The baseline 2030 scenario used the forecast that simply extended the current trend in growth at 1.3%. However, the largest of the six forecasts postulates a 1.8% growth rate resulting from more economic development than the current trend assumes. The high economic growth scenario uses this 1.8% growth rate in lieu of the 1.3%, but holds the rest of the ICIM configuration identical to the baseline 2030 scenario. Note that this means that installed capacity is designed around peak demand in 2030 that assumed 1.3% growth, but then is presented with a much higher demand for power.

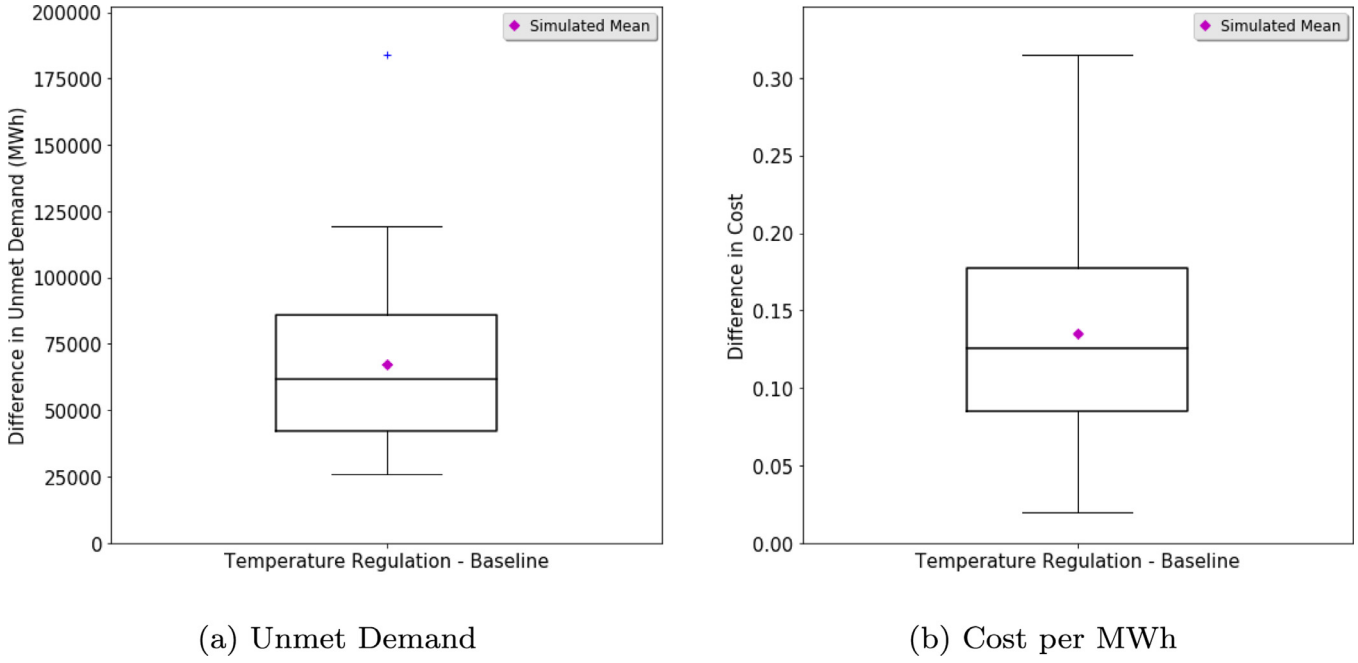

Fig. 20 – Temperature regulation compared to baseline 2030 ($n = 30$).

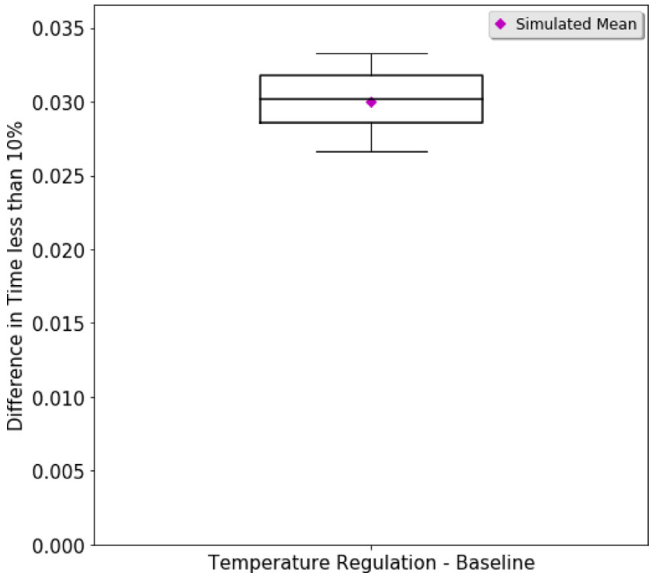

Fig. 21 – Temperature regulation compared to baseline of time less than 10% ($n = 30$).

Table 10 – Statistical differences in key metrics between temperature regulation and baseline 2030 scenarios.

Metric	Mean difference	95% Confidence interval	p-value
Unmet demand	67,109.8 MWh	(54133.0, 80086.6)	1.821×10^{-11}
Over supply	1798.9 MWh	(1406.7, 2191.0)	2.755×10^{-10}
Cost	\$0.13	(0.11, 0.16)	7.059×10^{-11}
Time less than 10%	3.0%	(2.9, 3.1)	$< 2.2 \times 10^{-16}$

Table 11 – Statistical differences in key metrics between high economic growth and baseline 2030 scenarios.

Metric	Mean difference	95% confidence interval	p-value
Unmet demand	181,604.9 MWh	(172815.7, 190394.1)	$< 2.2 \times 10^{-16}$
Cost	\$0.72	(0.65, 0.80)	$< 2.2 \times 10^{-16}$
Time less than 10%	12.0%	(12.0,12.2)	$< 2.2 \times 10^{-16}$

4.4.2. *High economic growth results*

Under the high economic growth scenario, the demand for power increases at a growth rate of 1.8% rather than 1.3%. In the unlikely event that long-term planners did not adjust to the higher growth rate during the intervening years, ICIM illustrates the impact these different economic assumptions would have on the baseline 2030 capacity plan. Fig. 22 shows the power demand curve overtaking the available capacity during the summer months. Note that the three factors are all significant: cost, unmet demand, and the percent of time the difference between demand and available capacity is less than 10%. However, over supply is not an issue as it was during the temperature regulation scenario. Table 11 gives the statistical difference comparison to the baseline 2030 scenario.

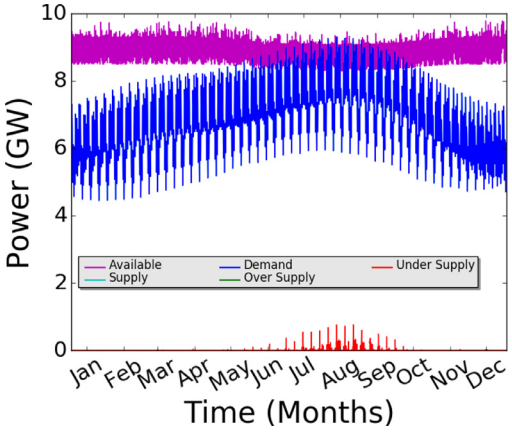

Fig. 22 – High economic growth scenario.

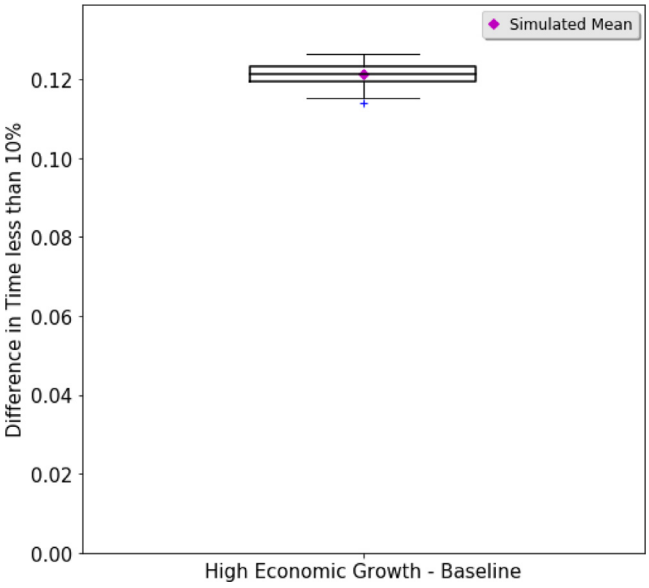

Fig. 24 – High economic growth compared to baseline of time less than 10% ($n = 30$).

4.5. *Extended drought scenario*

4.5.1. *Scenario description*

An additional concern in long-term planning is that future weather events may become more extreme. LCRA reported in 2015 that the region was experiencing a drought worse than drought of record that began in 2008 [45]. In 2011, LCRA experienced the lowest annual inflows the highland lakes ever recorded. The third and second lowest were 2013 and 2014, respectively. Reduced annual inflows leads to reduced combined storage and ultimately curtailment of water released from the highland lakes. The curtailment can in turn affect downstream power plants that depend on water levels remaining above their intake pipes to operate.

The extended drought scenario is designed to explore the impact of a drought worse than the one that started in 2008. The scenario assumes that the 2011 inflows—the lowest on record—persist for five consecutive years leading up to 2030. The previous experiments were compared to the baseline 2030 scenario, which is only one year. To provide a baseline comparator for the five-year drought scenario we configured ICIM to have all the installed capacity of electrical power that would exist by 2030. The water inflows were assumed to be the same as the years 2007 to 2011 while all other environmental variables were held the same as the baseline 2030 scenario. The power demand function incorporated a 1.3% growth rate such that 10 years of growth from 2015 to 2025

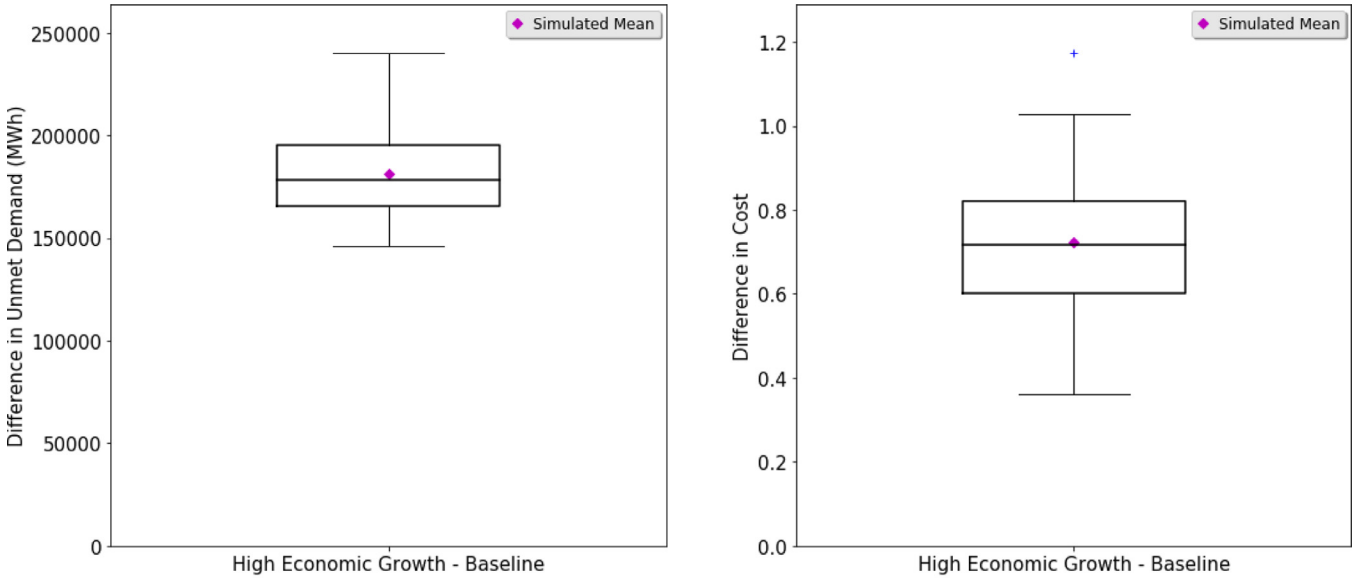

(a) Unmet Demand (b) Cost per MWh

Fig. 23 – High economic growth compared to baseline 2030 ($n = 30$).

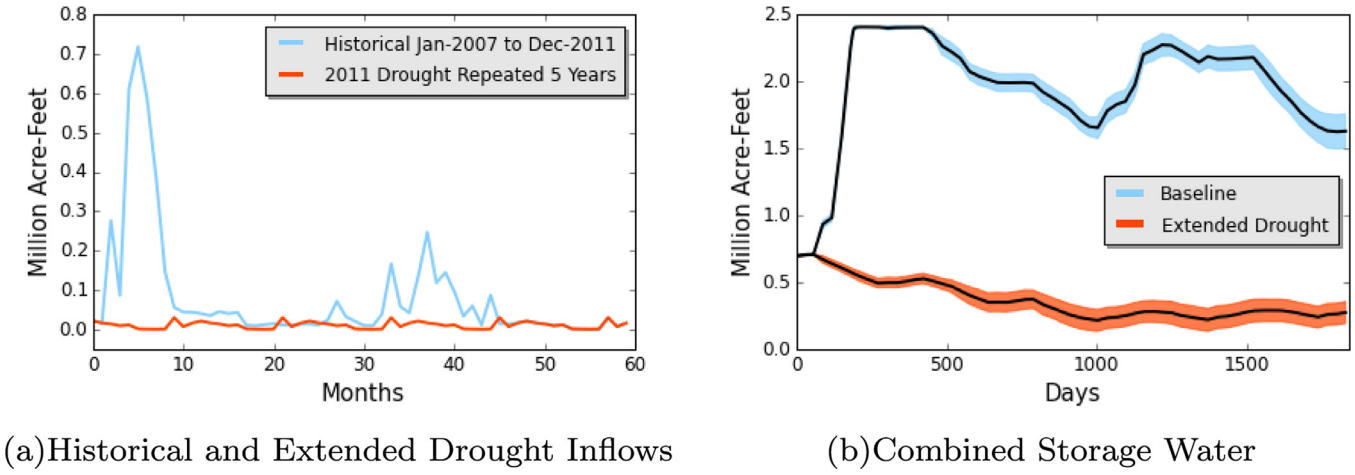

Fig. 25 – The five-year extended drought scenario.

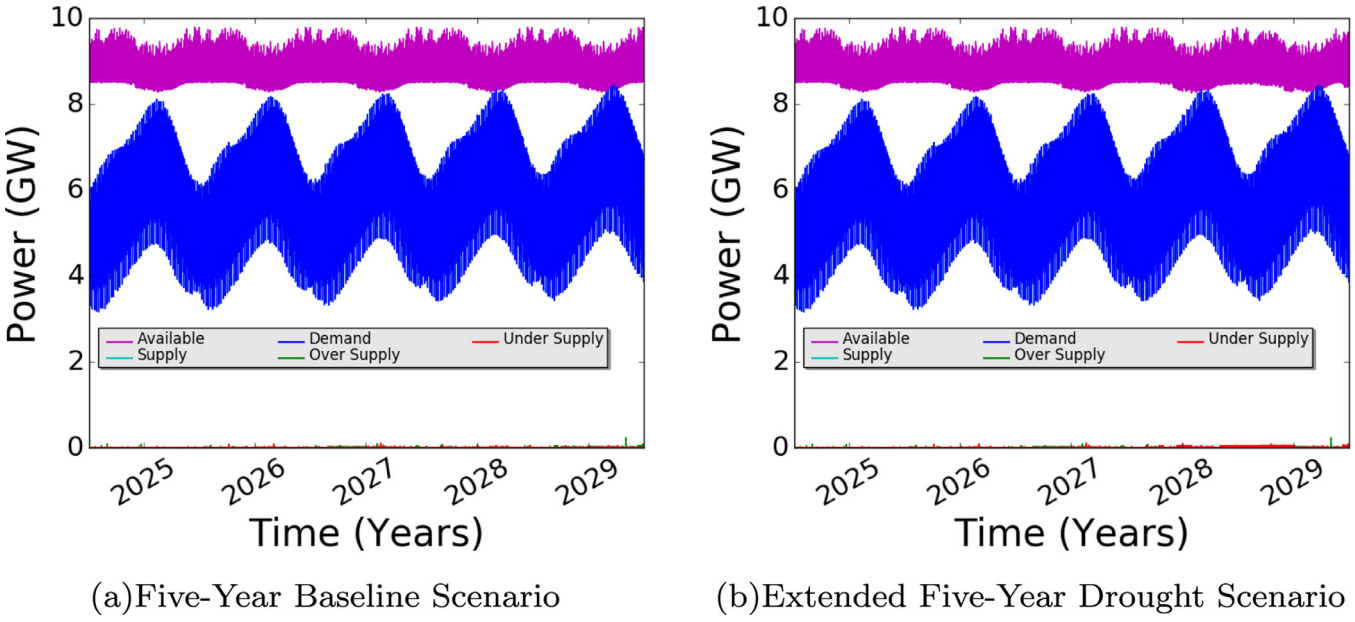

Fig. 26 – Power demand versus available capacity in the extended drought scenario.

were used to initialize the model, and then growth continued as the model ran from 2026 to 2030. The final year of this simulation run is thus equal to the baseline 2030 year used as the comparator for the other scenarios. The extended drought scenario simply substitutes the 2007 to 2011 inflows with the 2011 inflows repeated five times. Fig. 25 shows a comparison of the historical inflows from 2007 to 2011 overlaid on the 2011 inflows repeated five times, along with the calculated impact on combined storage over time.

4.5.2. *Extended drought results*

As discussed previously, the extended drought scenario requires a new baseline comparator to accommodate the five-year time line. Fig. 26 shows a replication from the five-year baseline and the comparable replication from the extended drought scenario. Although there were numerical differences between the five-year baseline and the extended drought scenario, the differences were statistically insignificant. However, certain replications within the batch of 30 performed under the extended drought conditions did experience large amounts of unmet demand. These large outliers are enough to skew the simulated mean up above 86,500 MWh, which is so much larger than the inter-quartile range that it is excluded from the box plot in Fig. 27(a). The occurrences were simply too infrequent to register statistically. Note this is largely due to the discrete nature of water intake pipes that draw cooling water for power generation. Low lake levels do not have a cumulative effect on power generation. The impact of lake levels occurs at the discrete moment when the level drops below the intake pipes. The fact that some replications crossed this threshold indicates the stress the system was under due to drought. Although the mean is statistically unchanged, the

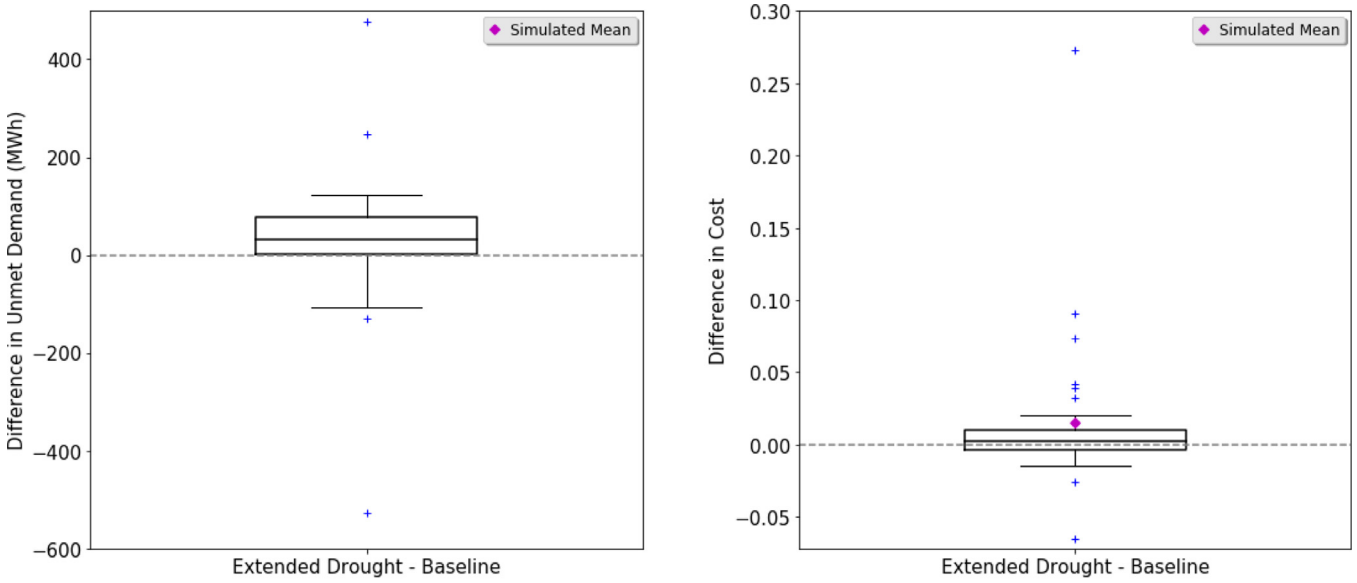

(a) Unmet Demand (b) Cost per MWh

Fig. 27 – Extended drought compared to baseline 2030 ($n = 30$).

Table 12 – Statistical differences in key metrics between extended drought and baseline 2030 scenarios.

Metric	Mean difference	95% confidence interval	p-value
Unmet demand	86,505.1 MWh	(−85620.2, 258630.4)	0.3125
Cost	$0.015	(−0.005, 0.037)	0.1379
Time less than 10%	1.0%	(−1.1, 3.2)	0.3294

study of outliers and their causes within the simulation can often provide useful insights for risk management in the face of extremely rare events.

4.6. *Lake loss scenario*

4.6.1. *Scenario description*

The final scenario explores the impact to a long-term plan in the extreme event that an entire lake becomes unusable. The reason for the lake loss is arbitrary, but might be due to some sort of contamination or some sort of sabotage of the water management equipment. The assumption is that plants that require cooling water from the lake are unable to operate until the lake is decontaminated or the system is repaired. The timing of the lake loss was picked to be the summer months when impact to the system would be largest.

4.6.2. *Lake loss results*

The results of a single replication of the lake loss scenario are shown in Fig. 29 for illustrative purposes. The impact of losing an entire lake is the most severe of the tested scenarios.

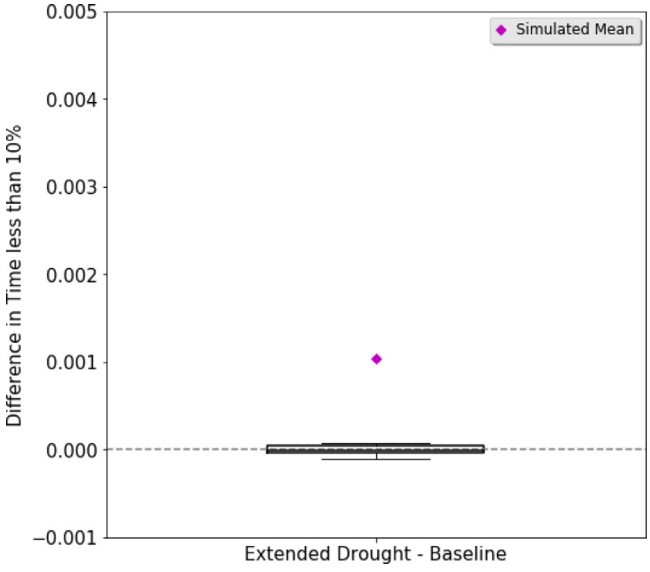

Fig. 28 – Extended drought compared to baseline of time less than 10% ($n = 30$).

Table 13 – Statistical differences in key metrics between lake loss and baseline 2030 scenarios.

Metric	Mean difference	95% confidence interval	p-value
Unmet Demand	1,873,706 MWh	(1847311, 1900102)	$< 2.2 \times 10^{-16}$
Cost	$5.34	(4.47, 6.22)	3.551×10^{-16}
Time less than 10%	17.51%	(17.39, 17.62)	$< 2.2 \times 10^{-16}$

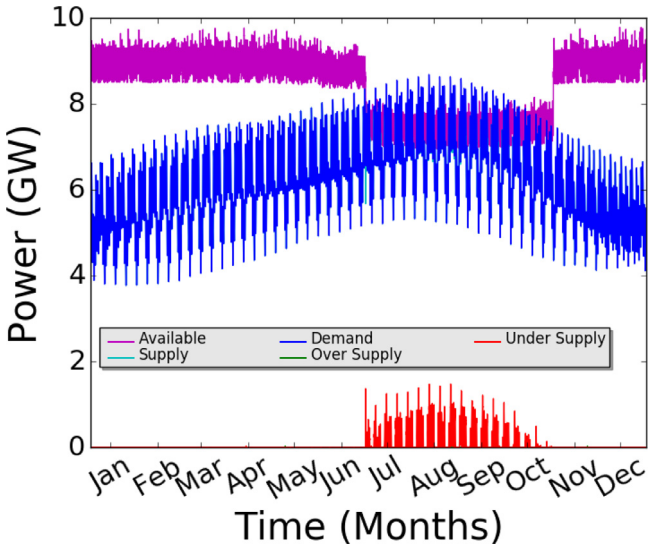

Fig. 29 – Lakeloss scenario results.

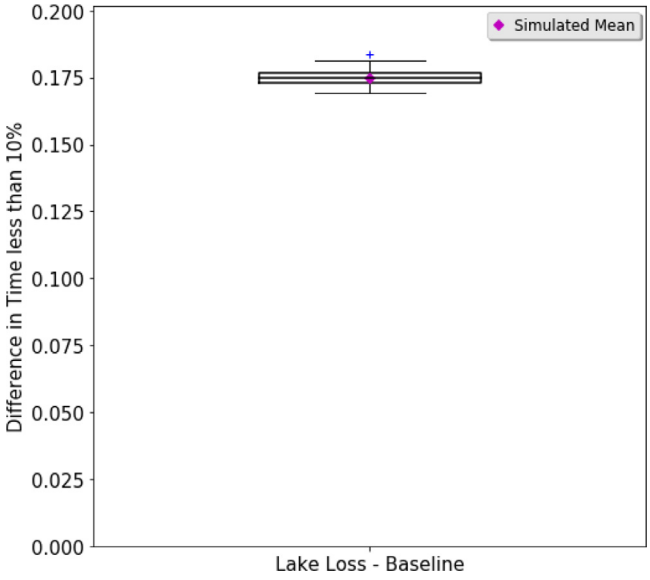

Fig. 31 – Lake loss compared to baseline of time less than 10% ($n = 30$).

Table 13 shows the statistical difference in cost, unmet demand, and percent of time available capacity was less than 10% above demand.

In water rich regions, such as LCRA, water temperature appears to have a greater impact on power generation than water availability (see Figs. 19 and 26). The highland lakes provide enough combined storage to withstand an extended drought worse than the current drought of record. However, this result cannot be generalized to other drought susceptible regions or other local scenarios, such as the loss of a lake due to contamination. It is possible that drought conditions could lead to more severe power loss than that experienced due to temperature changes. As previously mentioned, lake levels do not affect power generation in a cumulative manner, but rather there is a threshold that once crossed an entire plant may have to shut down. Conversely, water discharge temperature has a more gradual impact, reducing the amount of megawatt-hours that can be produced incrementally. The temperature regulation scenario in ICIM does indicate that state and federal water regulatory agencies should carefully consider the impact that water discharge temperature regula-

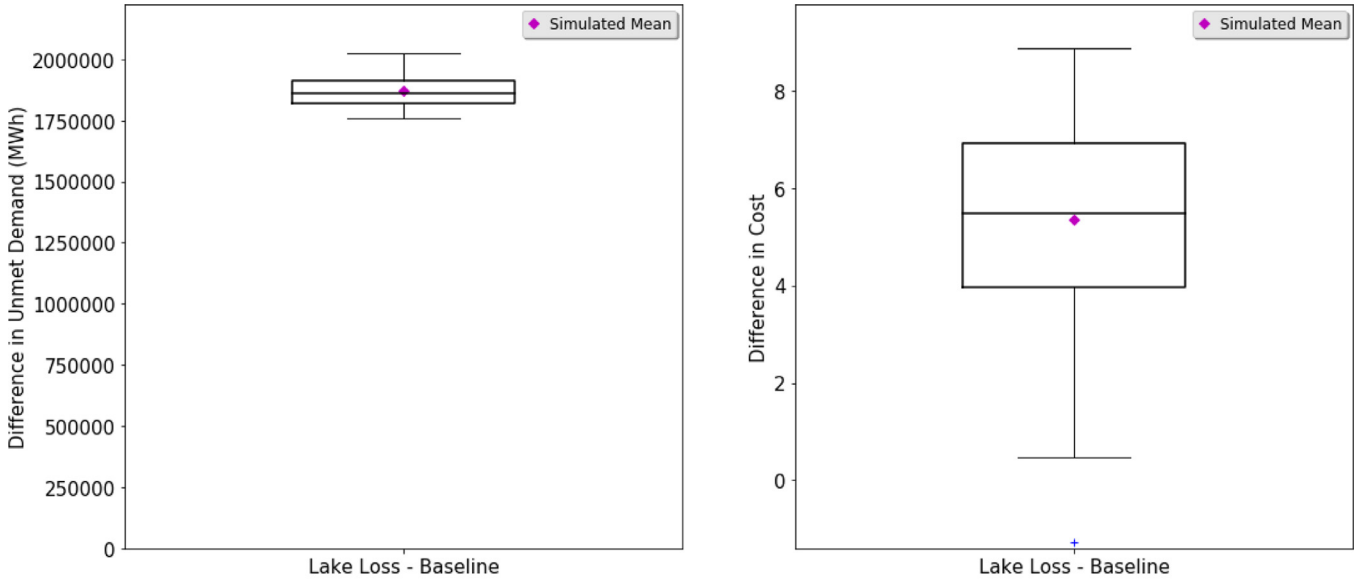

(a) Unmet Demand (b) Cost per MWh

Fig. 30 – Lakeloss compared to baseline 2030 ($n = 30$).

tions may have on power generation, especially during peak demand.

The preceding analysis suggests that regional power and water planners (e.g., ERCOT and LCRA) will want to factor future water temperatures and quantities into their power expansion plans. In particular, power planners should account for the impact of future water temperatures and quantities on both their existing installed capacity and future capacity expansions. Additionally, it seems obvious that drought susceptible regions of the U.S. should ensure their power and water agencies construct future plans together. Such joint planning should address both water withdrawals and returns for plant cooling at rivers and lakes and water consumption through evaporative heat removal in cooling ponds and wet towers. The amount of water actually consumed or contaminated to support future power generation capacity may affect the amount of water remaining for other societal uses.

5. Conclusions

ICIM demonstrates both the design and utility of an agent-based model in the long-term planning of interdependent critical infrastructures. By incorporating the plant-level decision-making process and the Independent System Operators' objective of minimizing the cost of power dispatched, we can capture both the aggregate measures of available capacity along with the granular measures of plant efficiency, adequate power generation, and relative cost per megawatt-hour. Additionally, we can begin to quantify the interdependence between power and water by incorporating water management agents with their own set of priorities, constraints, and management decisions. The impact of outlet temperature of cooling water and water consumption on power generation can be measured and different alternative scenarios can be compared.

As a result of the scenarios outlined in this report, we showed that:

1. Long-term capacity plans built from point estimates can be tested under stochastic conditions for robustness and resilience to uncertainty.
2. Uncertainty due to climate change can also be considered in conjunction with long-term plans and different levels of severity can be tested and compared.
3. Policy changes and regulations can be tested before they are implemented to identify possible unintended consequences.
4. The interdependency between power and water can be analyzed in terms of a region's ability to produce power and meet the demands of the community.

Regional and local power and water authorities can use the ICIM modeling paradigm described in this paper to identify potential shortfalls in meeting power and water demands in a region and test potential mitigation strategies that might address those shortfalls. While this has been demonstrated for LCRA, ICIM is easily expandable to other geographic regions of interest.

REFERENCES

[1] NIPP 2013: Partnering for critical infrastructure security and resilience, https://www.dhs.gov/national-infrastructure-protection-plan, accessed: 2017-08-03.
[2] R. Skaggs, K. Hibbard, T. Janetos, J. Rice, Climate and energy-water-land system interactions, Richland, WA.
[3] B. Bush, L. Dauelsberg, R. LeClaire, D. Powell, S. DeLand, M. Samsa, Three critical infrastructure protection decision support system (CIPP/DSS) project overview.
[4] G. L. Toole, A. W. McCown, Interdependent energy infrastructure simulation system, Wiley Handbook of Science and Technology for Homeland Security.
[5] T. McPherson, S. Burian, The water infrastructure simulation environment (wise) project, in: Impacts of Global Climate Change, 2005, pp. 1–8.
[6] J. Macknick, R. Newmark, G. Heath, K. Hallett, Operational water consumption and withdrawal factors for electricity generating technologies: A review of existing literature, Environmental Research Letters 7 (4) (2012) 045802.
[7] M. Chertoff, NIPP 2009: Partnering to enhance protection and resiliency, https://www.dhs.gov/xlibrary/assets/NIPP_Plan.pdf, accessed: 2017-08-03.
[8] J. R. Thompson, D. Frezza, B. Necioglu, M. Cohen, K. Hoffman, K. Rosfjord, An agent-based model for the evidence-based long term planning of power and water critical infrastructures, in: Systems Conference (SysCon), 2017 Annual IEEE International, IEEE, 2017, pp. 1–7.
[9] Fact sheet: Executive order (EO) 13636 improving critical infrastructure cybersecurity and presidential policy directive (PPD) 21 critical infrastructure security and resilience, https://www.dhs.gov/publication/eo-13636-ppd-21-fact-sheet, accessed: 2017-08-03.
[10] Energy sector specific plan 2015, https://www.dhs.gov/publication/nipp-ssp-energy-2015, accessed: 2017-08-03.
[11] National infrastructure protection plan-water2015, https://www.dhs.gov/publication/nipp-ssp-water-2015, accessed: 2017-08-03.
[12] F. Olsina, F. Garcés, H.-J. Haubrich, Modeling long-term dynamics of electricity markets, Energy Policy 34 (12) (2006) 1411–1433.
[13] S. A. Gabriel, A. S. Kydes, P. Whitman, The national energy modeling system: a large-scale energy-economic equilibrium model, Operations Research 49 (1) (2001) 14–25.
[14] C. Lenox, R. Dodder, C. Gage, O. Kaplan, D. Loughlin, W. Yelverton, EPA US nine-region markal database: database documentation (EPA/600/B-13/203), National Technical Information Service, Washington, DC.
[15] W. Short, N. Blair, P. Sullivan, T. Mai, Reeds model documentation: Base case data and model description, Golden, CO: National Renewable Energy Laboratory.
[16] J. Macknick, R. Newmark, G. Heath, K. Hallett, Operational water consumption and withdrawal factors for electricity generating technologies: a review of existing literature, Environmental Research Letters 7 (4) (2012) 045802.
[17] U. S. Energy Information Agency, Form EIA-860 detailed data, accessed: 2017-08-25 (2015).
[18] B. R. Scanlon, I. Duncan, R. C. Reedy, Drought and the water–energy nexus in Texas, Environmental Research Letters 8 (4) (2013) 045033.
[19] 2014 Long-term System Assessment for the ERCOT Region, http://www.brattle.com/system/news/pdf2s/000/000/793/original/2014_Long-Term_System_Assessment_for_the_ERCOT_Region.pdf?1423847967, accessed: 2017-08-25.

[20] Stakeholder-driven scenario development for the ERCOT 2014 long-term system assessment, http://www.brattle.com/system/publications/pdfs/000/005/094/original/Stakeholder-Driven_Scenario_Development_for_the_ERCOT.pdf?1418752741, accessed: 2017-08-25.
[21] Report on the capacity, demand and reserves in the ERCOT region 2018-2027, http://www.ercot.com/content/wcm/lists/114798/CapacityDemandandReserveReport-May2017.pdf, accessed: 2017-08-25.
[22] Priorities for the evolution of an energy only electricity market design in ERCOT, https://sites.hks.harvard.edu/fs/whogan/Hogan_Pope_ERCOT_050917.pdf, accessed: 2017-08-25.
[23] N. Nakicenovic, R. Swart, Special report on emissions scenarios, Edited by Nebojsa Nakicenovic and Robert Swart, pp. 612. ISBN 0521804930. Cambridge, UK: Cambridge University Press, July 2000.
[24] P. Stier, J. Feichter, S. Kinne, S. Kloster, E. Vignati, J. Wilson, L. Ganzeveld, I. Tegen, M. Werner, Y. Balkanski, et al., The aerosol-climate model echam5-ham, Atmospheric Chemistry and Physics 5 (4) (2005) 1125–1156.
[25] D. Salas-Mélia, F. Chauvin, M. Déqué, H. Douville, J. Gueremy, P. Marquet, S. Planton, J. Royer, S. Tyteca, Description and validation of the cnrm-cm3 global coupled model, CNRM W'orking Note 103 (2005) 36.
[26] O. Marti, P. Braconnot, J. Bellier, R. Benshila, S. Bony, P. Brockmann, P. Cadule, A. Caubel, S. Denvil, J. Dufresne, et al., The new ipsl climate system model: Ipsl-cm4, Note du Pôle de Modélisation, IPSL 26 (2005) 1–86.
[27] X. Liang, D. P. Lettenmaier, E. F. Wood, S. J. Burges, A simple hydrologically based model of land surface water and energy fluxes for general circulation models, Journal of Geophysical Research: Atmospheres 99 (D7) (1994) 14415–14428.
[28] D. Lohmann, R. NOLTE-HOLUBE, E. Raschke, A large-scale horizontal routing model to be coupled to land surface parametrization schemes, Tellus A 48 (5) (1996) 708–721.
[29] D. E. Prudic, L. F. Konikow, E. R. Banta, A new streamflow-routing (sfr1) package to simulate stream-aquifer interaction with modflow-2000, Tech. rep. (2004).
[30] J. R. Yearsley, A semi-lagrangian water temperature model for advection-dominated river systems, Water Resources Research 45 (12).
[31] M. T. Van Vliet, J. R. Yearsley, F. Ludwig, S. Vögele, D. P. Lettenmaier, P. Kabat, Vulnerability of US and European electricity supply to climate change, Nature Climate Change 2 (9) (2012) 676–681.
[32] J. H. Miller, S. E. Page, Complex Adaptive Systems: An Introduction to Computational Models of Social Life, Princeton University Press, 2009.
[33] S. M. Rinaldi, J. P. Peerenboom, T. K. Kelly, Identifying, understanding, and analyzing critical infrastructure interdependencies, IEEE Control Systems 21 (6) (2001) 11–25.
[34] M. Ouyang, Review on modeling and simulation of interdependent critical infrastructure systems, Reliability engineering & System safety 121 (2014) 43–60.
[35] J. M. Epstein, R. Axtell, Growing artificial societies: social science from the bottom up, Brookings Institution Press, 1996.
[36] D. C. Barton, E. D. Eidson, D. A. Schoenwald, K. L. Stamber, R. K. Reinert, Aspen-ee: an agent-based model of infrastructure interdependency, SAND2000-2925. Albuquerque, NM: Sandia National Laboratories.
[37] T. Veselka, G. Boyd, G. Conzelmann, V. Koritarov, C. Macal, M. North, B. Schoepfle, P. Thimmapuram, Simulating the behavior of electricity markets with an agent-based methodology: the electric market complex adaptive systems (EMCAS) model, Argonne National Laboratory.
[38] J. Sun, L. Tesfatsion, Dynamic testing of wholesale power market designs: An open-source agent-based framework, Computational Economics 30 (3) (2007) 291–327.
[39] J. M. Galán, A. López-Paredes, R. Del Olmo, An agent-based model for domestic water management in Valladolid metropolitan area, Water Resources Research 45 (5).
[40] V. Rai, A. D. Henry, Agent-based modelling of consumer energy choices, Nature Climate Change 6 (6) (2016) 556.
[41] D. R. Biggar, M. R. Hesamzadeh, The Economics of Electricity Markets, John Wiley & Sons, 2014.
[42] Lakes Buchanan and Travis water management plan and drought contingency plans, https://www.lcra.org/water/water-supply/water-management-plan-for-lower-colorado-river-basin/Documents/FINAL-WMP-AsApprovedbyTCEQ-Nov-2015.pdf, accessed: 2017-08-25.
[43] R. H. Shumway, D. S. Stoffer, Time series analysis and its applications, Studies In Informatics And Control 9 (4) (2000) 375–376.
[44] Report on the capacity, demand and reserves (CDR) in the ERCOT region, 2018-2027, http://www.ercot.com/content/wcm/lists/.../CapacityDemandandReserveReport-May2017.pdf, accessed: 2017-09-27.
[45] Historic drought and the Lower Colorado River Basin, https://www.lcra.org/water/water-supply/highland-lakes-overview/Documents/Fact-Sheet-General-Drought.pdf, accessed: 2017-09-28.